Table 1 Distribution of three forms of AFM images in various reaction products

	Control	U100 DNA	Control + Pol B1	U100 DNA + Pol B1	Control + Pol B1 + dNTPs + primer	U100 DNA + Pol B1 + dNTPs + primer
ssDNA	87.5 (300)	91.3 (95)	80.8 (84)	81.6 (129)	34.1 (30)	61.2 (123)
Other Forms*	12.5 (43)	8.7 (9)	14.4 (15)	18.4 (29)	40.9 (36)	34.3 (69)
dsDNA	0 (0)	0 (0)	4.8 (5)	0 (0)	25.0 (22)	4.5 (9)

Data are percentages of each form, i.e. ssDNA, dsDNA and other forms, relative to the total number of forms. The percentage and number (in parentheses) of each form are presented. For "Control (or U100 DNA) + Pol B1 + dNTPs +Primer" experiments, the reaction conditions are the same as those described in Experimental procedures. For "Control (or U100 DNA) +Pol B 1" experiments, R2 and F1 primers and dNTPs were omitted from the reaction mixture. For "Control or U100 DNA" experiments, PolB1, R2 and F1 primers and dNTPs were omitted from the mixture. *Other forms include the intermediate where Pol B1 appeared to bind to DNA. In these experiments, the ratio of Pol B1 (1 pmol) and ssDNA (control or U100 DNA, 2 pmol) in the reaction mixture (40 μL) was 1 : 2 (see Experimental procedures). The ratio of the enzyme (20 pmol) and ssDNA (0.1 pmol) in the reaction mixture (20 μL) was 200 : 1 for *in vitro* DNA synthesis where extensive digestion of U100 DNA was observed (Fig. 2).

length of 1.4 kb DNA (0.32 nm × 1400 = 448 nm). The reaction mixtures containing Pol B1, ssDNA (Control or U100 DNA), primers and dNTPs were subjected to AFM analysis before and after incubation for 15 min at 55 °C (Fig. 4B). There were many Form I (ssDNA) and Form III (Pol B1) molecules in the mixtures before the incubation. After the incubation, however, Form II (dsDNA) became apparent in the reaction mixtures containing control DNA. In contrast, Form II (dsDNA) was rare in the mixtures containing U100 DNA, and other forms such as those where Pol B1 appeared to bind to DNA were noted (Form IV, Fig. 4A,C). The sizes of the bound molecules (50–70 nm) were similar to those of monomeric forms of Pol B1 (Fig. 4A,D).

To analyze the dsDNA formation more quantitatively, individual molecules on the mica were counted, and the percentage of each form among total molecules was calculated (Table 1). It is evident that Form II (dsDNA) was generated, concomitant with the reduction of the number of Form I (ssDNA) in the reaction mixture containing control DNA, Pol B1, primers and dNTPs. The number of Form II (dsDNA) increased to a quarter of the total number of molecules (22/88 total molecules) while that of Form I (ssDNA) decreased to one third of it (30/88 total molecules). In contrast, Form II (dsDNA) accounted for only 5% of the total number of molecules (9/201 total molecules) and Form I (ssDNA) represented more than 60% (123/201 total molecules) in reaction mixtures containing U100 DNA, Pol B1, primers and dNTPs. The differences in the distribution of each form between two reaction products were statistically significant ($P < 0.0001$ by χ^2 test). These results confirm the inhibitory effects of template uracil on DNA synthesis by Pol B1. Form IV (DNA plus Pol B1) accounted for about 41% (36/88 total molecules) and 34% (69/201 total molecules), respectively, of total numbers of molecules in the two reaction products. These values are significantly larger than the percentages of Form IV observed in the samples of Control (13% = 43/343), U100 DNA (9% = 9/104), Control DNA plus Pol B1 (14% = 15/104) and U100 DNA plus Pol B1 (18% = 29/158), suggesting that DNA synthesis accelerates the formation of Form IV.

Discussion

Uracil is one of the most ubiquitously occurring mutagenic damages in DNA (Lindahl 1993). It is generated by deamination of cytosine in DNA as well as by incorporation of dUTP into DNA by DNA polymerases (Vassylyev & Morikawa 1996). Since the deamination of cytosine results in G:U base pairs, and the uracil in template DNA directs DNA polymerases to incorporate adenine opposite it, the hydrolytic reaction can convert original G:C base pairs to A:T base pairs in a half of the progeny. To exclude uracil from DNA, organisms possess various uracil-DNA glycosylases, which specifically excise uracil in DNA (Pearl 2000), and dUTPases, which hydrolyze dUTP to dUMP plus PPi to maintain low levels of dUTP in the cellular nucleotide pool (Hogrefe

et al. 2002). In addition, hyperthermophilic archaeal B family DNA polymerases such as Pol B1 or Pfu possess unique mechanisms that recognize uracil in template DNA and inhibit the progress of DNA synthesis upstream from the lesion (Greagg *et al.* 1999). Given the genotoxicity of uracil in DNA, the recognition mechanism by the polymerases appears to contribute to the maintenance of genome integrity of the organisms living in the habitats at high temperatures.

To better understand the binding mechanisms, we examined the binding modes of Pol B1 to uracil in DNA by gel mobility shift assays and atomic force microscopy. We used the same ssDNA substrates, i.e. control and U100 DNA, whose molecular sizes are 1.4 kb, throughout the analyses. These DNAs were chosen because the linear form of dsDNA (Form II) can be clearly visible with AFM and is distinct from Form III (Pol B1). In addition, the ssDNA is efficiently converted to dsDNA by Pol B1 within 10 min at 55 °C (Fig. 2). The efficient conversion from ssDNA to dsDNA suggests that the ssDNA does not form substantial intramolecular base interactions at 55 °C, thereby allowing the progress of DNA polymerase on the template strand. Although Pol B1 itself could specifically bind to ssDNA containing uracil, the molar ratio between ssDNA containing uracil (U100 DNA) and Pol B1 required for the band shift was 1 : 200 in the absence of DNA synthesis (Fig. 1). The presence of uracil in the ssDNA strongly inhibited DNA syntheses by Pol B1 and Pfu exo$^-$ but not by Taq DNA polymerases (Fig. 2). The inhibitory effect was also clearly observed when the formation of dsDNA (Form II) in reaction products containing U100 DNA in the presence of Pol B1, primers and dNTPs was analyzed by atomic force microscopy (Table 1). The percentage of dsDNA was significantly lower in the reaction mixture containing U100 DNA (5%) than in that containing control DNA (25%).

Since the presence of uracil in DNA strongly inhibits the DNA synthesis by DNA pol B1, we postulated DNA pol B1 might bind to uracil in DNA in the progress of DNA synthesis more efficiently compared to during random diffusion in solution. Interestingly, the binding efficiency of Pol B1 to uracil was greatly enhanced by initiating DNA synthesis (Fig. 3). The molar ratio between U100 DNA and Pol B1 was 1 : 10 when the reaction mixtures contained primers and dNTPs necessary for DNA synthesis. Thus, we suggested that Pol B1 binds more efficiently to uracil when it proceeds along with template DNA for DNA synthesis rather than during random collision with DNA in solution (Fig. 5). This conclusion is consistent with the result that the percentage of Form IV (DNA plus DNA pol B1) in the mixture containing DNA pol B1 and U100 DNA was significantly higher in the presence of DNA synthesis (34%) than in the absence (18%) (Table 1). As described in the Introduction, the expression level of Pol B1 is 1500 molecules per cell, which is noticeably higher than the ones reported for *E. coli* DNA polymerases (Gruz *et al.* 2003). Because of the preferential binding of Pol B1 to uracil during DNA synthesis, we suggest that the majority of Pol B1 molecules are engaged in DNA replication and recognize uracil during DNA synthesis rather than directly binding to uracil in the non-replicating chromosome as lesion-specific binding proteins. Since Pol B1 is less sensitive in sensing uracil in the template strand than Pfu exo$^-$ (Gruz *et al.* 2003), which binds tightly to uracil in template/primer DNA (Shuttleworth *et al.* 2004), we suggest that Pol B1 might continue DNA synthesis beyond template uracil to some extent and randomly halt replication before template uracil along with template DNA (Fig. 5). In fact, we observed Pol B1 bound to uracil-containing DNA at various positions in the template DNA. It should be noted that Pol B1 possesses 3′ to 5′ exonuclease activity (Pisani & Rossi 1994). Thus, the primer strand may be digested at least in part when Pol B1 encounters uracil in template DNA during DNA synthesis *in vivo*.

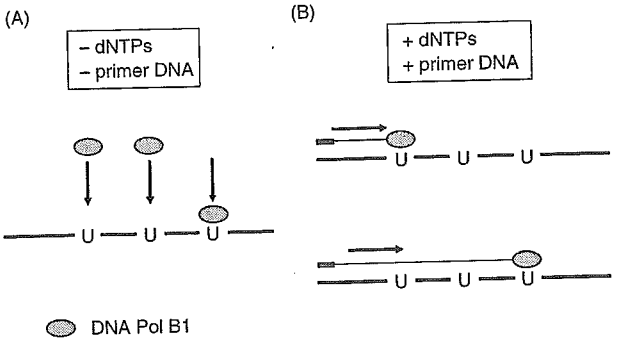

Figure 5 Schematic model of the mechanism of recognition of uracil in DNA by Pol B1. (A) Random diffusion-mediated recognition. Pol B1 randomly diffuses in solution and binds to uracil in DNA. (B) DNA replication-mediated recognition. Pol B1 slides on template DNA for elongation of primer and binds to uracil in DNA.

Since archaeal DNA polymerases bind to uracil-containing ssDNA, it is possible that one polymerase molecule actively extending the primer is blocked by a second polymerase bound to uracil in the template strand (Greagg *et al.* 1999). This "blocking" model seems plausible in particular for the long-range primer extension, and contrasts with the "read-ahead" model where single molecules of DNA polymerases directly bind to uracil in the template DNA and stop replication. To distinguish the two possibilities, we used AFM and suggested that Pol B1 bound to uracil-containing DNA as a monomeric

form (Fig. 4). This finding directly supports the "read-ahead" model as a mechanism by which archaeal DNA polymerases halt copying DNA before template uracil. Since Form IV (DNA plus DNA pol B1) was observed even in "Control" or "U 100 DNA" samples where no Pol B1 was added, some of Form IV observed were not necessarily true replication intermediates where DNA polymerases bound to DNA. However, Form IV was more frequently generated when DNA replication was initiated (Table 1). Thus, we suggest that a significant portion of Form IV observed in the samples of "Control + Pol B1 + dNTPs + Primer" and "U100 DNA + Pol B1 + dNTPs +Primer" include the true replication intermediates. The sizes of the molecules bound to control DNA and U100 DNA in the presence of dNTPs and primers were indistinguishable. Hence, we suggested that monomeric forms of Pol B1 bind to uracil in template DNA. However, more extensive quantification of the size of many of the blobs at the end of the dsDNA in different conditions is needed for the final conclusion.

Both Pol B1 and Pfu exo$^-$ bind not only to template uracil but also to template hypoxanthine, a deamination product of adenine (Gruz *et al.* 2003). Pfu exo$^-$ stalls three to four bps before hypoxanthine as well as uracil in the template strand, and Pol B1 displays a similar stalling behavior. Hypoxanthine pairs with cytosine during DNA replication and induces A:T to G:C transitions if not repaired. Thus, this stalling behavior seems to suppress the incorporation of cytosine opposite template hypoxanthine, thereby reducing the mutagenic potential of hypoxanthine. Stalling Pol B1 at template uracil or hypoxanthine may generate ss gap DNA region downstream of the lesions. Recombination that seals the gap with DNA sequence of sister chromatid or translesion DNA synthesis with Y-family DNA polymerase may contribute to the gap filling (Fig. 6). In fact, *Sulfolobus solfataricus* possesses a homolog of Rad51, i.e. RadA, a recombination protein, and a homolog of *E. coli* DNA pol IV, i.e. *Sso* DNA pol Y1 or Dpo4, a Y-family DNA polymerase(Seitz *et al.* 1998; Gruz *et al.* 2001; Ohmori *et al.* 2001; She *et al.* 2001). In addition, it has uracil DNA glycosylase to excise uracil in DNA (She *et al.* 2001). Thus, it is important to investigate how these proteins are involved in the subsequent steps leading to repair of deaminated bases in archaeal DNA.

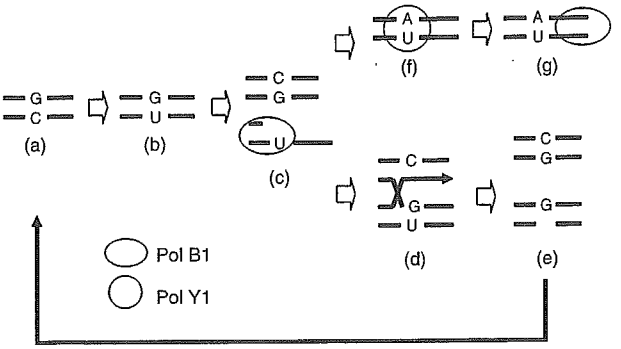

Figure 6 Possible mechanisms by which daughter strand gaps generated by stalling of Pol B1 at template uracil (or hypoxanthine) are sealed by homologous recombination and/or translesion bypass by Pol Y1. Cytosine in DNA (a) is deaminated by heat, thereby generating G:U mismatch (b). When the strand containing uracil is copied by Pol B1 before the uracil is removed by repair enzymes, Pol B1 may stop before uracil (c). ssDNA region downstream of the uracil can be sealed by homologous recombination with DNA sequence from sister chromatid (d). Uracil DNA glycosylase may excise the uracil (e) and provides a chance to regenerate normal G:C bp (a). However, if Pol B1 is switched to Pol Y1, the Y-family DNA polymerase may bypass uracil by incorporating adenine opposite template uracil (f). Then, another polymerase switch occurs and Pol B1 extends the primer strand containing adenine opposite uracil, thereby generating a mutagenic mispair in DNA (g).

Experimental procedures

Preparation of ssDNAs with or without uracil

TaKaRa Taq DNA polymerase, Pfu DNA polymerase exo$^-$, and FPLC-grade dNTPs were purchased from TaKaRa (Shiga, Japan), Stratagene (La Jolla, CA, USA) and Amersham Biosciences, respectively. Pol B1 was purified as previously described (Pisani & Rossi 1994). About 1.4 kb DNA was amplified by PCR using plasmid pUC118 DNA (3.2 kb), F1-biotin primer (5′ biotin-GGGAGAAAGGCGGACAGGTA-3′, 20 pmol), R2 primer (5′-GGCTGGCTTAACTATGCGGC-3′, 20 pmol), Taq DNA polymerase (1 unit) and four dNTPs (4 nmol each) in a total volume of 20 μL. Taq DNA polymerase almost equally incorporates dUTP and dTTP opposite template adenine (Lasken *et al.* 1996). Advantage was taken of this property and 1.4 kb DNA containing uracil was prepared by the same PCR conditions except for the presence of dUTP (4 nmol) instead of dTTP. The former and latter amplified DNAs were named "control DNA" and "U100 DNA," respectively. After the amplification, excess primers were digested with ssDNA specific exonuclease, i.e. ExoSAP-IT (Amersham Biosciences). The proteins were inactivated by heat and proteinase K treatments, and removed by phenol/chloroform/isoamylalcohol extraction. The DNAs were purified by ethanol precipitation, and re-suspended in TE buffer. After removal of low-molecular-weight contaminants by filtration with Microcon YM100 (Millipore, Bedford, MA, USA), ssDNAs were prepared by heating (100 °C × 5 min) followed by rapid cooling on ice. The resulting ssDNAs were used for the analysis with AFM. ssDNAs for gel shift assays were prepared with magnetic streptavidin bead according to the manufacturer's protocol (MAGNOTEX-SA, TaKaRa, Japan). Briefly, the filtrated DNAs having biotin were mixed with MAGNOTEX-SA, and ssDNAs without biotin

were obtained in the supernatant after treatments with alkaline solution. The incorporation of uracil into DNA was confirmed by treating the DNAs with uracil DNA glycosylase (Gibco BRL, Gaithersburg, MD, USA), which converts uracil into abasic sites in DNA (Krokan *et al.* 2002). U100 DNA, but not control DNA, became a poor substrate for PCR amplification with Taq because of the generation of abasic sites.

Gel mobility shift assay

Interactions between Pol B1 and ssDNA with or without uracil were examined under various conditions, the details of which are described in the legends of Figs 1–4. Briefly, the reaction mixture (20 μL) contained 10 mM Tris-HCl (pH 8.3), 50 mM KCl and 1.5 mM $MgCl_2$ (Tris/KCl/$MgCl_2$). In addition, it contained F1 primer (5′-GGGAGAAAGGCGGACAGGTA-3′), four dNTPs, Pol B1 and ssDNA. When the interactions were analyzed without DNA synthesis, F1 primer and dNTPs were omitted from the mixture. The reaction was carried out at 55 °C and terminated by the addition of 1/10 volume of 40 mM ethylenediaminetetraacetic acid (EDTA) solution. The reaction products were separated by electrophoresis with 1% agarose gel, and transferred to nylon membrane (Hybond-N+, Amersham Biosciences) for Southern hybridization analysis. Probe DNA (0.7 kb) was prepared by PCR in a reaction mixture containing pUC118, F1 primer and R1 primer (5′-GGCCTCT-TCGCTATTACGCC-3′). R1 primer anneals a DNA sequence close to the multiple-cloning site of pUC118, while F1 and R2 primers anneal DNA sequences each 0.7 kb apart from the cloning site in opposite directions. The amplified DNA was fluorescently labeled and used for the hybridization with ECL Direct Nucleic Acid Labeling and Detection System (Amersham Biosciences). The hybridized DNA was quantified using a chemiluminescent detection system, i.e. ChemiDoc (Bio-Rad, Richmond, CA, USA).

AFM analysis

The reaction mixture (40 μL) contained 10 mM Tris-HCl (pH 8.3), 50 mM KCl, 1.5 mM $MgCl_2$, 20 pmol each of R2 and F1 primers, 8 nmol each of four dNTPs, 1 pmol Pol B1 and 2 pmol of ssDNA (control or U100 DNA). The reaction was carried out for 15 min at 55 °C, and the samples were directly deposited on to freshly cleaved and discharged mica, followed by a rinse with distilled water and blown dry with dry nitrogen. The plates were placed in a desiccator for 1 h before analysis. The samples were visualized with AFM (Model SPI 3800 N, Seiko Instruments Inc., Japan) in dynamic force mode (DFM) operation with a 20 μm scanner (Murakami *et al.* 2000, 2001). The cantilevers for the DFM-AFM (Micro Cantilever, Type SI-DF40, Seiko Instruments Inc., Japan) were used for the analysis. Images were collected at room temperature. Scan frequencies were typically 2.0 Hz, and all images contain 512 × 512 data points.

Acknowledgements

Part of this study was financially supported by the Budget for Nuclear Research of the Ministry of Education, Culture, Sports, Science and Technology, Japan, based on the screening and counseling by the Atomic Energy Commission. This work was also supported by Grants-in-aid for Cancer Research from the Ministry of Health, Labour and Welfare, Japan, and for International Collaborative Research from the Japan Health Science Foundation.

References

Argaman, M., Golan, R., Thomson, N.H. & Hansma, H.G. (1997) Phase imaging of moving DNA molecules and DNA molecules replicated in the atomic force microscope. *Nucleic Acids Res.* **25**, 4379–4384.

De Felice, M., Sensen, C.W., Charlebois, R.L., Rossi, M. & Pisani, F.M. (1999) Two DNA polymerase sliding clamps from the thermophilic archaeon Sulfolobus solfataricus. *J. Mol. Biol.* **291**, 47–57.

Engel, A. & Muller, D.J. (2000) Observing single biomolecules at work with the atomic force microscope. *Nature Struct. Biol.* **7**, 715–718.

Fogg, M.J., Pearl, L.H. & Connolly, B.A. (2002) Structural basis for uracil recognition by archaeal family B DNA polymerases. *Nature Struct. Biol.* **9**, 922–927.

Greagg, M.A., Fogg, M.J., Panayotou, G., Evans, S.J., Connolly, B.A. & Pearl, L.H. (1999) A read-ahead function in archaeal DNA polymerases detects promutagenic template-strand uracil. *Proc. Natl. Acad. Sci. USA* **96**, 9045–9050.

Grogan, D.W., Carver, G.T. & Drake, J.W. (2001) Genetic fidelity under harsh conditions: analysis of spontaneous mutation in the thermoacidophilic archaeon Sulfolobus acidocaldarius. *Proc. Natl. Acad. Sci. USA* **98**, 7928–7933.

Gruz, P., Pisani, F.M., Shimizu, M., *et al.* (2001) Synthetic activity of Sso DNA polymerase Y1, an archaeal DinB-like DNA polymerase, is stimulated by processivity factors proliferating cell nuclear antigen and replication factor C. *J. Biol. Chem.* **276**, 47394–47401.

Gruz, P., Shimizu, M., Pisani, F.M., De Felice, M., Kanke, Y. & Nohmi, T. (2003) Processing of DNA lesions by archaeal DNA polymerases from Sulfolobus solfataricus. *Nucleic Acids Res.* **31**, 4024–4030.

Hogrefe, H.H., Hansen, C.J., Scott, B.R. & Nielson, K.B. (2002) Archaeal dUTPase enhances PCR amplifications with archaeal DNA polymerases by preventing dUTP incorporation. *Proc. Natl. Acad. Sci. USA* **99**, 596–601.

Krokan, H.E., Drablos, F. & Slupphaug, G. (2002) Uracil in DNA—occurrence, consequences and repair. *Oncogene* **21**, 8935–8948.

Lasken, R.S., Schuster, D.M. & Rashtchian, A. (1996) Archaebacterial DNA polymerases tightly bind uracil-containing DNA. *J. Biol. Chem.* **271**, 17692–17696.

Lindahl, T. (1993) Instability and decay of the primary structure of DNA. *Nature* **362**, 709–715.

Lindahl, T. & Nyberg, B. (1974) Heat-induced deamination of cytosine residues in deoxyribonucleic acid. *Biochemistry* **13**, 3405–3410.

Murakami, M., Hirokawa, H. & Hayata, I. (2000) Analysis of radiation damage of DNA by atomic force microscopy in

comparison with agarose gel electrophoresis studies. *J. Biochem. Biophys. Meth* **44**, 31–40.

Murakami, M., Minamihisamatsu, M., Sato, K. & Hayata, I. (2001) Structural analysis of heavy ion radiation-induced chromosome aberrations by atomic force microscopy. *J. Biochem. Biophys. Meth* **48**, 293–301.

Ohmori, H., Friedberg, E.C., Fuchs, R.P., *et al.* (2001) The Y-family of DNA polymerases. *Mol. Cell* **8**, 7–8.

Pearl, L.H. (2000) Structure and function in the uracil-DNA glycosylase superfamily. *Mutat. Res.* **460**, 165–181.

Pisani, F.M. & Rossi, M. (1994) Evidence that an archaeal alpha-like DNA polymerase has a modular organization of its associated catalytic activities. *J. Biol. Chem.* **269**, 7887–7892.

Sartori, A.A., Fitz-Gibbon, S., Yang, H., Miller, J.H. & Jiricny, J. (2002) A novel uracil-DNA glycosylase with broad substrate specificity and an unusual active site. *EMBO J.* **21**, 3182–3191.

Seitz, E.M., Brockman, J.P., Sandler, S.J., Clark, A.J. & Kowalczykowski, S.C. (1998) RadA protein is an archaeal RecA protein homolog that catalyzes DNA strand exchange. *Genes Dev.* **12**, 1248–1253.

She, Q., Singh, R.K., Confalonieri, F., *et al.* (2001) The complete genome of the crenarchaeon Sulfolobus solfataricus P2. *Proc. Natl. Acad. Sci. USA* **98**, 7835–7840.

Shuttleworth, G., Fogg, M.J., Kurpiewski, M.R., Jen-Jacobson, L. & Connolly, B.A. (2004) Recognition of the pro-mutagenic base uracil by family B DNA polymerases from archaea. *J. Mol. Biol.* **337**, 621–634.

Vassylyev, D.G. & Morikawa, K. (1996) Precluding uracil from DNA. *Structure* **4**, 1381–1385.

Received: 10 July 2005
Accepted: 3 October 2005

Structures and Biological Properties of DNA Adducts Derived from *N*-Nitroso Bile Acid Conjugates

Yukari Totsuka,*,† Rena Nishigaki,† Shigeki Enomoto,† Takeji Takamura-Enya,† Ken-ichi Masumura,‡ Takehiko Nohmi,‡ Nobuo Kawahara,‡ Takashi Sugimura,† and Keiji Wakabayashi†

Cancer Prevention Basic Research Project, National Cancer Center Research Institute, 1-1 Tsukiji 5-chome, Chuo-ku, Tokyo 104-0045, Japan, and National Institute of Health Sciences, 1-18-1 Kamiyoga, Setagaya-ku, Tokyo 158-0098, Japan

Received June 3, 2005

A kind of *N*-nitrosobile acid conjugate, *N*-nitrosotaurocholic acid (NO-TCA), was incubated with calf thymus DNA, and formation of an adduct was detected by the ^{32}P-postlabeling method under nuclease P1 conditions. To examine the nucleotides containing the adduct from NO-TCA, each of 2′-deoxyribonucleotide 3′-monophosphates (3′-dAp, 3′-dGp, 3′-dCp, or 3′-Tp) was incubated with NO-TCA. The same adduct spot was detected in the reaction of NO-TCA with 3′-dCp. The structure of this adduct was determined to be 3-ethanesulfonic acid-dC by several spectrometry techniques. Moreover, bulky adducts containing bile acid moiety were also produced from the reaction of NO-TCA with 3′-dCp and 3′-dAp. From comparison with spectral data for authentic compounds, these adducts were concluded to be N^4-cholyl-dC and N^6-cholyl-dA. N^4-Cholyl-dC and N^6-cholyl-dA were also detected in calf thymus DNA treated with NO-TCA. In addition, 3-ethanesulfonic acid-dC and N^4-deoxycholyl-dC were found to be produced from *N*-nitrosotaurodeoxycholic acid (NO-TDCA) with dC. NO-TCA and NO-TDCA induced mutations in *Salmonella typhimurium* TA100 but not in TA98. Mutational spectrum analysis revealed that NO-TCA induced G to A transitions predominantly. When NO-TCA (250 mg/kg) was singly administered to male Wistar rats by gavage, both ethanesulfonic acid-dC and N^4-cholyl-dC could be detected in the glandular stomach and colon. The levels of ethanesulfonic acid-dC were 0.22−0.29 per 10^6 nucleotides, but values for N^4-cholyl-dC were about 500-fold lower. These observations suggest that *N*-nitroso bile acid conjugates, NO-TCA and NO-TDCA, may induce G to A base substitutions in genes via DNA adduct formation, producing ethanesulfonic acid- and/or (deoxy)cholic acid-DNA and, therefore, may be related to human carcinogenesis as endogenous mutagens.

Introduction

Epidemiological studies have indicated an association between bile acids and colorectal cancer (*1*, *2*), and high levels of secondary bile acids are present in the feces of populations at high risk of colorectal cancer (*3*, *4*). It has further been reported that deoxycholic acid (DCA)[1] stimulates proliferation of colonic epithelium in vitro and in vivo (*5*, *6*) and suppresses not only spontaneous but also butyrate-induced apoptosis in human colonic adenoma cells in vitro (*7*). In addition, bile acids or bile acid conjugates, such as cholic acid (CA), chenodeoxycholic acid (CDCA), litocholic acid (LCA), and taurodeoxycholic acid (TDCA), promote development of colorectal adenomas and adenocarcinomas in rats (*8*, *9*). There is some evidence of formation of DNA adducts with bile acids in vitro (*10*−*13*).

N-Nitroso bile acid conjugates, such as *N*-nitrosoglycocholic acid (NO-GCA) and *N*-nitrosotaurocholic acid (NO-TCA), have already been demonstrated to exert mutagenic activity in both bacterial and mammalian assay systems (*14*, *15*). Moreover, these compounds also can induce liver and stomach cancers in F344 rats (*16*). *N*-Nitroso bile acid conjugates are also thought to be among the presumed carcinogens of stomach and esophageal tumor development in rat duodenogastoric reflux models (*17*−*19*). For this purpose, rats are subjected to surgery in order to induce duodenal reflux into the stomach or the esophagus, thus being chronically exposed to the mixture of duodenal and gastric juice. After 50 weeks of such exposure, adenocarcinomas are found in the digestive tract without exogenous carcinogens, at reported incidences of 31−41% for stomach and 44% for esophagus. In general, patients undergoing distal gastrectomy have been reported to be at increased risk of gastric carcinoma (*20*, *21*). It has been shown that the risk is higher after Billroth II rather than Billroth I resection (*20*, *22*, *23*), the difference reflecting levels of duodenogastric reflux. The amounts of bile acid conjugates in humans are reported to be 16−40 mg/mL in bile juice, 0.08−6.77 mg/mL in gastric juices from patients

* To whom correspondence should be addressed. Tel: +81-3-3547-5201 (ext. 4353). Fax: +80-3-3543-9305. E-mail: ytotsuka@gan2.res.ncc.go.jp.
† National Cancer Center Research Institute.
‡ National Institute of Health Sciences.

[1] Abbreviations: DCA, deoxycholic acid; CA, cholic acid; CDCA, chenodeoxycholic acid; LCA, litocholic acid; NO-GCA, *N*-nitrosoglycocholic acid; NO-TCA, *N*-nitrosotaurocholic acid; NO-TDCA, *N*-nitrosotaurodeoxycholic acid; 3′-dAp, 2′-deoxyadenosine 3′-monophosphate; 3′-dGp, 2′-deoxyguanosine 3′-monophosphate; 3′-dCp, 2′-deoxycitidine 3′-monophosphate; 3′-Tp, thymidine 3′-monophosphate; dA, 2′-deoxyadenosine; dG, 2′-deoxyguanosine; dC, 2′-deoxycitidine; dT, 2′-deoxytymidine; N^4-cholyl-dC, N^4-cholyl-2′-deoxycytidine; N^6-cholyl-dA, N^6-cholyl-2′-deoxyadenosine; PEI, polyethyleneimine; T4-PNK, T4-polynucleotide kinase.

10.1021/tx050144x CCC: $30.25
Published on Web 09/14/2005

with bile reflux gastritis, and 0.29−3.45 μg/mL in serum (*24*, *25*). Because intragastric formation of nitrosamides could be mediated by acid-catalyzed reaction of amides with nitrite, *N*-nitroso compounds have been suggested as plausible etiological factors in development of gastric cancer in humans (*26*, *27*). In fact, it has also been reported that taurocholic acid (TCA) is nitrosated in simulated gastric juice (*14*). Moreover, thioproline, an effective nitrite-trapping agent, could inhibit the development of esophageal adenocarcinoma induced by gastroduodenal reflux in rats (*19*). Such nitrosation is also suggested to be mediated by activated macrophages in infected and inflamed organs. Therefore, it is likely that nitrosated bile acid conjugates could contribute to cancer development as endogenous mutagens.

It is reported that O^6-carboxymethyl-guanine, 7-carboxymethyl-guanine, and 3-carboxymethyl-adenine are produced in vitro when *N*-nitrosoglycocholic acid (NO-GCA) is incubated with calf thymus DNA under neutral conditions (*28*). Similarly, it is suggested that *N*-nitrosotauroursodeoxycholic acid would form ethane sulfonic acid-DNA; however, the structure is not fully known yet (*27*). Moreover, little is known about the formation of bulky adducts containing bile acid moieties; we recently found that bile acid-DNA adducts could be formed by the reaction of DNA with cholyl adenylate, a reactive intermediate in the production of bile acid-amino acid conjugates. Structural analyses determined these bile acid-DNA adducts to be N^4-cholyl-2′-deoxycytidine (N^4-cholyl-dC) and N^6-cholyl-2′-deoxyadenosine (N^6-cholyl-dA) (*29*). Therefore, it is possible that similar bile acid-DNA adducts might be formed from *N*-nitroso bile acid conjugates. In the present study, we investigated the formation and chemical structures of DNA adducts containing ethane sulfonic acid and bile acid moieties, produced by the reaction of *N*-nitroso bile acid conjugates, NO-TCA, and *N*-nitrosotaurodeoxycholic acid (NO-TDCA), with DNA. Moreover, mutagenic activities of *N*-nitroso bile acid conjugates and their mutation spectra in *Salmonella typhimurium* TA100 were also examined. We also report here the formation of DNA adducts in some tissues of rats administered NO-TCA. From these results, the biological significance of NO-TCA and NO-TDCA as endogenous mutagens is discussed.

Materials and Methods

Materials. NO-TCA and NO-TDCA were obtained from the Nard Institute (Osaka, Japan). 2′-Deoxyribonucleotide 3′-monophosphate (3′-dAp, 3′-dGp, 3′-dCp, and 3′-Tp) and 2′-deoxyribonucleoside (dA, dG, dC, and T) were from Sigma Chemical Co. (St. Louis, MO). Micrococcal nuclease and phosphodiesterase II were purchased from Worthington Biochemical Co. (Freehold, NJ). [γ-^{32}P]ATP, T4 polynucleotidekinase (T4-PNK), nuclease P1, and phosphodiesterase I were obtained from ICN Biochemicals (Irvine, CA), Takara Shuzo Co. (Kyoto, Japan), Yamasa Shoyu Co. (Choshi, Japan), and Worthington Biochemical Co., respectively. All other chemicals used were of analytical grade.

Spectral Measurements. ^{1}H NMR spectra were recorded with JEOLGX-α600 or α800 instruments using microprobe FT-NMR spectrometers. Electronspray ionization mass spectrometry (ESI-MS) was performed using a Waters ZQ 2000 mass spectrometer equipped with an Agilent 1100 HPLC system. UV absorbance spectra were measured on a PD-8020 photodiode array detector (Tosoh, Tokyo, Japan).

Chemical Synthesis of N^4-Cholyl-dC and N^6-Cholyl-dA. Authentic N^4-cholyl-dC and N^6-cholyl-dA were synthesized according to the procedure reported previously (*29*). Briefly, 3′,5′-bis-*O*-*tert*-butyldimethylsilyl-2′-deoxycitiydine (0.1 mmol) or 3′,5′-bis-*O*-*tert*-butyldimethylsilyl-2′-deoxyadenosine (0.1 mmol) was stirred with CA (0.1 mmol) and dicyclohexylcarbodiimide (0.12 mmol) in pyridine at 70 °C for 4 h. The organic phase was evaporated, and then, these residues were separated on column chromatography, followed by deprotection.

Reaction of *N*-Nitrosobile Acid Conjugates and Nucleotide and/or DNA. Ten micromole aliquots of each *N*-nitrosobile acid conjugate (NO-TCA or NO-TDCA) were incubated with 650 nmol of calf thymus DNA in 1 mL of 100 mM phosphate buffer (pH 7.4) at 37 °C for 24 h. Then, DNA was extracted with phenol/chloroform:isoamyl alcohol (24:1 v/v) and precipitated with ethanol. DNA concentrations were measured spectrophotometrically at 260 nm and adjusted to 2 mg/mL in 0.01× SSC buffer. With reactions between *N*-nitrosobile acid conjugates and mononucleotides, 650 nmol of each 2′-deoxyribonucleotide 3′-monophosphate (3′-dAp, 3′-dGp, 3′-dCp, and 3′-Tp) was used instead of calf thymus DNA. Adduct formation was analyzed by the ^{32}P-postlabeling method under nuclease P1 conditions as described below.

Structural Analysis of Ethane Sulfonic Acid-dC Adducts. NO-TCA or NO-TDCA was incubated with dC in 100 mM phosphate buffer (pH 7.4) at 37 °C for 24 h, and the resulting solution was separated by HPLC as follows. An aliquot of the solution was applied to a semipreparative Capcell pack C18 column (5 μm particle size, 10 mm × 250 mm; Shiseido, Tokyo, Japan), and a mobile phase of 2% acetonitrile in 0.25% triethylamine-acetic acid (pH 6.3) was pumped in isocratically at a flow rate of 3 mL/min. In addition to a few peaks detected in the solution without dC, a peak, eluting at a retention time of 9.3 min, was newly observed in the reaction mixture of NO-TCA and dC. The peak was collected and injected into an analytical grade TSKgel ODS-80Ts column (5 μm particle size, 4.6 mm × 250 mm; Tosoh) for further purification. The applied material was eluted at a flow rate of 1 mL/min with a gradient system of 2.5% methanol in 0.1% heptafluorobutylic acid (pH 3.0) for 10 min and then a linear gradient to 80% methanol in 0.1% heptafluorobutylic acid. All of the above HPLC procedures were performed several times at an ambient temperature with monitoring of eluate at 254 nm. The compound was collected for determination of UV absorption, mass, and ^{1}H and ^{13}C NMR spectra. ^{1}H and ^{13}C NMR spectrum assignment of the adduct was performed with DQF-COSY, HMQC, and HMBC. The following data were obtained.

^{1}H NMR (DMSO-d_6): δ 8.09 [d, J = 7.2, H-6 (dC), 1H], 6.11 [d, J = 7.2, H-5 (dC), 1H], 6.07 [t, J = 6.4, H-1′ (dR), 1H], 5.29 [d, J = 4.0, H-3′-OH (dR), 1H], 5.07 [t, J = 4.8, H-5′-OH (dR), 1H], 4.21−4.19 [m, H-3′ (dR), 1H], 4.15 (dd, J = 7.2, 6.4, H-$\underline{CH_2}CH_2SO_3H$, 2H), 3.83 [dd, J = 7.2, 3.2, H-4′ (dR), 1H], 3.61−3.59 [m, H-5″ (dR), 1H], 3.57−3.54 [m, H-5′ (dR), 1H], 2.86 (t, J = 6.4, H-$CH_2\underline{CH_2}SO_3H$, 2H), 2.23−2.21 [m, H-2″ (dR), 1H], 2.13−2.10 [m, H-2′ (dR), 1H]. ^{13}C NMR (DMSO-d_6) δ 159.1 [C-4 (dC)], 147.6 [C-2 (dC)], 140.6 [C-6 (dC)], 95.2 [C-5 (dC)], 88.0 [C-4′ (dR)], 86.6 [C-1′ (dR)], 69.6 [C-3′ (dR)], 60.7 [C-5′ (dR)], 47.1 (C-$CH_2\underline{CH_2}SO_3H$), 41.1 (C-$\underline{CH_2}CH_2SO_3H$). ESI-MS *m/z* 334, 218. UV λ_{max} 219, 280 nm.

Structural Analysis of CA-dC Adducts. NO-TCA was incubated with dC, and the solution was subjected to HPLC under the following conditions. An aliquot was applied to an analytical grade TSKgel ODS-80Ts column (5 μm particle size, 4.6 mm × 250 mm; Tosoh) and eluted at a flow rate of 1 mL/min with a linear gradient of acetonitrile (from 20 to 80%) in 0.1% diethylamine-acetic acid (pH 6.0) over 30 min. In addition to a few peaks detected in the solution without dC, a peak, eluted at a retention time of 21.3 min, was observed in the reaction mixture of NO-TCA and dC. UV absorption and mass spectra showed absorption maxima at 245 and 298 nm and molecular ion peaks at *m/z* 502 and 618. From comparison with the UV and mass spectra for authentic N^4-cholyl-dC, the compound at a peak of 21.3 min was suggested to be a CA-dC adduct. The peak fraction was therefore collected and applied to ^{1}H NMR spectral analyses. The following data were obtained.

^{1}H NMR (DMSO-d_6): δ 10.81 (s, 1H, NHCO), 8.30 [d, J = 7.2, 1H, H-6 (dC)], 7.21 [d, J = 7.2, 1H, H-5 (dC)], 6.09 [t, J = 6.4, 1H, H-1′ (dR)], 5.27 [brs, 1H, 3′-OH (dR)], 5.04 [brs, 1H, 5′-OH (dR)], 4.31 [s, 1H, 3-OH (CA)], 4.20 [brs, 1H, H-3′ (dR)], 4.11 [d, J = 3.2, 1H, 12-OH (CA)], 4.00 [d, J = 3.2, 1H, 7-OH (CA)], 3.84 [dd, J = 7.2, 3.6, 1H, H-4′ (dR)], 3.77 [d, J = 2.8, 1H, H-12 (CA)], 3.60−3.54 [m, 3H, H-7 (CA), H-5′, 5″ (dR)], 3.50−3.17 [m, 1H, H-3 (CA) overlapped with the absorbance signal of H_2O], 2.30−2.13 [m, 5H, H-4α, 9, 23α, 23β (CA), H-2′ (dR)], 2.01−1.98 [m, 2H, H-14 (CA), H-2″ (dR)], 1.79−1.62 [m, 7H, H-17, 20, 22α, 16α, 1α, 6β, 15β (CA)], 1.45−1.14 [m, 12H, H-2α, 2β, 4β, 5, 6α, 8, 11α, 11β, 15α, 16β, 22β (CA)], 0.98−0.92 [m, 4H, H-1β, CH_3-21 (CA)], 0.80 [s, 3H, CH_3-19 (CA)], 0.57 [s, 3H, CH_3-18 (CA)]. ESI-MS *m/z* 618, 502. UV λ_{max} 245, 298 nm.

Structural Analysis of CA-dA Adducts. NO-TCA was incubated with dA as described above and separated by HPLC under the same conditions as for structural analysis of CA-dC adducts. A peak eluting at a retention time of 15.4 min was observed in the reaction mixture, and the UV absorption pattern showed absorption maximum at 273 nm. Because the HPLC eluting position and UV spectrum of the compound were similar to those of the authentic N^6-cholyl-dA, this compound was deduced to be a CA-dA adduct. LC-ESI/MS analysis demonstrated this compound to exhibit a molecular ion at *m/z* 642 and fragment at *m/z* 526, the latter deriving from loss of deoxyribose. Therefore, the chemical structure of the compound was concluded to be N^6-cholyl-dA.

Structural Analysis of DCA-dC Adducts. NO-TDCA and dC were incubated in 100 mM phosphate buffer (pH 7.4) at 37 °C for 24 h and separated by HPLC according to the same procedure as for CA-dC or dA adducts. A peak showing a similar UV absorption pattern to N^4-cholyl-dC was observed at a retention time of 23.0 min and collected for UV, mass, and ^{1}H and ^{13}C NMR spectral analyses. ^{1}H and ^{13}C NMR spectrum assignment of the adduct was conducted with DQF-COSY, HMQC, and HMBC. The following data were obtained.

^{1}H NMR (DMSO-d_6): δ 10.81 (s, 1H, NHCO), 8.30 [d, J = 7.2, 1H, H-6 (dC)], 7.20 [d, J = 7.2, 1H, H-5 (dC)], 6.09 [t, J = 6.2, 1H, H-1′ (dR)], 5.27 [brs, 1H, 3′-OH (dR)], 5.04 [brs, 1H, 5′-OH (dR)], 4.45 [s, 1H, 3-OH (DCA)], 4.20 [brs, 1H, H-3′ (dR)], 3.84 [dd, J = 6.6, 2.4, 1H, H-4′ (dR)], 3.77 [brs, 1H, H-12 (DCA)], 3.59−3.56 [m, 3H, H-7 (DCA), H-5′, 5″ (dR)], 3.50−3.17 [m, 1H, H-3 (DCA)], 2.40−2.25 [m, 5H, H-4α, 9, 23α, 23β (DCA), H-2′ (dR)], 2.02−1.96 [m, 2H, H-14 (DCA), H-2″ (dR)], 1.80−1.44 [m, 8H, H-17, 20, 22α, 16α, 1α, 6β, 7β, 15β (DCA)], 1.35−1.15 [m, 13H, H-2α, 2β, 4β, 5, 6α, 7α, 8, 11α, 11β, 15α, 16β, 22β (DCA)], 1.09−0.91 [m, 4H, H-1β, CH_3-21 (DCA)], 0.83 [s, 3H, CH_3-19 (DCA)], 0.58 [s, 3H, CH_3-18 (DCA)]. ^{13}C NMR (DMSO-d_6): δ 175.0 [C=O (DCA)], 162.9 [C-4 (dC)], 155.0 [C-2 (dC, C=O)], 145.5 [C-6 (dC)], 95.8 [C-5 (dC)], 88.5 [C-4′ (dR)], 86.7 [C-1′ (dR)], 71.6 [C-12 (DCA)], 70.5 [C-3 (DCA), C-3′ (dR)], 61.5 [C-5′ (dR)], 47.4 [C-14 (DCA)], 46.3 [C-17 (DCA)], 46.0 [C-13 (DCA)], 41.6 [C-5 (DCA)], 40.9 [C-2′ (dR)], 40−39 [C-4, 8 (DCA) overlapped with absorbance signal of DMSO], 36.3 [C-23 (DCA)], 35.1 [C-1 (DCA)], 35.0 [C-20 (DCA)], 33.8 [C-10 (DCA)], 32.9 [C-9 (DCA)], 30.9 [C-22 (DCA)], 30.2 [C-2 (DCA)], 28.6 [C-11 (DCA)], 27.1 [C-16 (DCA)], 27.0 [C-6 (DCA)], 26.1 [C-7 (DCA)], 23.5 [C-15 (DCA)], 23.1 [C-19 (DCA)], 17.0 [C-21 (DCA)], 12.5 [C-18 (DCA)]. ESI-MS *m/z* 602, 486. UV λ_{max} 246, 298 nm.

Analysis of DNA Adducts Derived from Bile Acid Conjugates in the Organs of Rats Administered NO-TCA. Five male Wistar rats, purchased from Charles River Japan, Inc. (Atsugi, Japan), were provided with food (CE-2 pellet diet, CLEA Japan) and tap water ad libitum. NO-TCA was dissolved in water and administered to three rats as a single oral dose by gavage at level of 250 mg per kg body wt. The two rats in the control group received the solvent alone. At 24 h after administration of NO-TCA, both chemically treated and control groups of rats were euthanized under ether anesthesia. The major organs, such as the liver, glandular stomach, and colon mucosa, were excised and stored at −80 °C until DNA extraction by a standard procedure with enzymatic digestion of protein and RNA followed by extraction with phenol and chloroform/isoamyl alcohol (24:1, v/v). The experiments were conducted according to the Guidelines for Animal Experiments in National Cancer Center of the Committee for Ethics of Animal Experimentation of the National Cancer Center.

Enzymatic digests of 100 μg aliquots of DNA were subjected to HPLC using the heptafulorobutylic acid-methanol system as described in the structure analysis of 3-ethane sulfonic acid-dC, and the eluents were collected at retention times of 3−4 min for analysis of 3-ethanesulfonic acid-dC and 46−47 min for analysis of N^4-cholyl-dC. The retention times for 3-ethanesulfonic acid-3′-dCp and N^4-cholyl-3′-dCp were confirmed using LC-ESI/MS analysis. After lyophilization of the fractioned samples, residues were dissolved in 10 μL of distilled water and then subjected to ^{32}P-postlabeling analysis under nuclease P1 conditions, as described below.

^{32}P-Postlabeling Method. DNA obtained from the in vitro experiments using calf thymus DNA or the in vivo experiments was digested with micrococcal nuclease and phosphodiesterase II and then ^{32}P-postlabeled using the nuclease P1 enrichment method as reported previously (*30*). For the in vitro experiments using deoxyribonucleotide 3′-monophosphate as a DNA source, ^{32}P-postlabeling was performed under nuclease P1 conditions without DNA digestion.

For the separation of ethanesulfonic acid-DNA adduct, the resulting ^{32}P-postlabeled samples were applied to a polyethyleneimine (PEI) cellulose TLC sheet (POLYGRAM CEL 300 PEI; Macherey-Nagel, Duren, Germany), attached to 10 cm filter paper at the top, and developed with 0.1 M lithium chloride, 3 M acetic acid, and 3 M urea to remove [^{32}P]phosphate and [γ-^{32}P]ATP, as previously reported (*31*).

For the analysis of CA-DNA adducts, the ^{32}P-postlabeled samples were applied to a PEI-cellulose sheet, attached to 10 cm filter paper at the top, and developed with 2.3 M sodium phosphate buffer (pH 6.0) to remove normal nucleotides. The modified nucleotides remaining at the origin were contact-transferred to another PEI-cellulose sheet and then subjected to two-dimensional TLC. The solvent system for development consisted of buffer A (2.07 M lithium formate and 7.65 M urea, pH 3.5) from bottom to top and buffer B (0.90 M lithium chloride, 0.45 M Tris-HCl, and 7.65 M urea, pH 8.0) from left to right, followed by 1.7 M sodium phosphate buffer, pH 6.0, from left to right, with 3.5 cm filter paper.

Adducts were detected with a Bio-Image Analyzer (BAS 2000; Fuji Photo Film Co., Tokyo, Japan) after exposing the TLC sheets to Fuji imaging plates or autoradiography on Kodak XAR-5 film with intensifying screens. Relative adduct labeling was determined by the methods of Gupta et al. (*32*) and Reddy et al. (*30*), and values were calculated as averages using data from three assays.

Mutagenicity Assay. The preincubation method (*33*) was carried out for testing the mutagenicity of *N*-nitrosobile acid conjugates to *S. typhimurium* TA98 and TA100. Briefly, bacterial cells were incubated with the test chemical without S9 mix for 20 min at 37 °C in a total volume of 0.7 mL. The mixture was poured onto agar plates with 2 mL of soft agar and incubated for 2 days at 37 °C. The numbers of His$^+$ revertants per plate were then determined.

Sequencing of *hisG46* Mutations. A 201 bp DNA fragment containing the *hisG46* site was amplified by colony PCR (forward primer: 5′-GAT TGA TAT CCT GCG CGT GCG TG-3′; reverse primer: 5′-TCG TCA ACC GGT GTT GCC AGC G-3′). DNA sequencing was performed with a BigDye Terminater Cycle Sequencing Kit (Applied Biosystems, Foster City, CA) on an ABI PRISM 310 Genetic Analyzer (Applied Biosystems).

Results

Formation of Ethane Sulfonic Acid-dC Adduct by NO-TCA. In reactions of NO-GCA with DNA, 7-carboxymethylguanine and O^6-methylguanine are reported

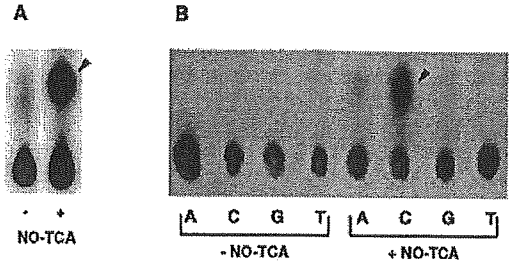

Figure 1. Autoradiogram of ethanesulfonic acid-DNA adducts derived from NO-TCA. Calf thymus DNA (A) or each of 2′-deoxyribonucleotide 3′-monophosphate (B) was incubated with or without NO-TCA, and DNA adduct formation was analyzed by ^{32}P-postlabeling under nuclease P1 conditions. The adduct spots are indicated by the arrowheads.

to be produced, thus taurine-modified DNA adduct is expected to be formed from NO-TCA (*27*, *28*). Therefore, NO-TCA was incubated with 650 nmol of calf thymus DNA under neutral conditions at 37 °C for 24 h and adduct formation was analyzed by ^{32}P-postlabeling under nuclease P1 conditions. TLC development was carried out with 0.1 M lithium chloride, 3 M acetic acid, and 3 M urea, as previously reported, being different from the TLC development systems for bulky adduct (*30*). As shown in Figure 1A, radioactive spots were detected at the origin in the mixture without NO-TCA, but one spot, in an upper position from the origin, was clearly observed in the reaction mixture of NO-TCA and calf thymus DNA. The adduct level was estimated to be 30.2 ± 6.21 per 10^5 nucleotides. To examine the nucleotides involved in the adducts with NO-TCA treatment, the compound was incubated with separate 2′-deoxyribonucleotide 3′-monophosphate (3′-dAp, 3′-dGp, 3′-dCp, and 3′-dTp), and adduct formation was analyzed. As shown in Figure 1B, the same adduct was also detected in the reaction of NO-TCA with 3′-dCp.

To analyze its chemical structure, NO-TCA was incubated with dC and the resulting solution was separated by HPLC. An aliquot of the solution was applied to a semipreparative ODS column, and a peak, eluting at a retention time of 9.3 min, was observed. This peak fraction was then further purified using an analytical grade ODS column, and a peak eluting at a retention time of 9.5 min was collected for analyses of UV absorption, mass, and ^{1}H and ^{13}C NMR spectra. The yield of this adduct from dC was about 1%. Its UV/vis absorption spectrum showed absorption maxima at 280 nm (Figure 2), and mass spectrum analysis revealed a molecular ion at *m/z* 334 corresponding to a protonated derivative of the conjugated product of ethanesulfonic acid and deoxycytidine and a fragmentation ion at *m/z* 218, consistent with loss of the deoxyribose moiety. Figure 3 shows the ^{1}H NMR spectrum of ethanesulfonic acid-dC compound measured in DMSO-d_6. The 15 protons were assigned with DQF-COSY, HMQC, and HMBC. The proton signals corresponding to the 2′-deoxycytidine moiety [H-1′, 2′, 2″, 3′, 4′, 5′, 5″, 3′-OH, 5′-OH (dR), H-5, -6 (dC)] were observed from 2.10 to 8.09 ppm. Moreover, proton signals at 4.15 and 2.86 ppm were assigned to the ethanesulfonic acid moiety. Although no proton signal was observed corresponding to the exocyclic amino group, the N4 position of the cytidine, HMBC analysis showed the signal at 4.15 ppm on ^{1}H NMR spectroscopy of the ethanesulfonic acid moiety to clearly correlate with signal peaks at 159.1 and 147.6 ppm in the ^{13}C NMR spectrum

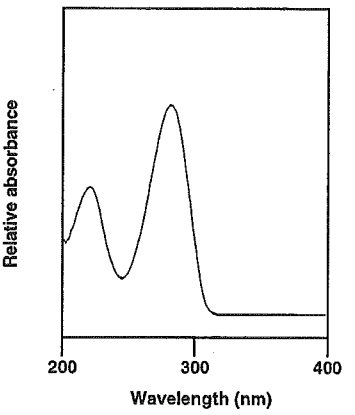

Figure 2. UV/vis absorption spectrum of the ethansulfonic acid-dC adduct. An aliquot of the reaction mixture of NO-TCA and dC was applied to HPLC on an analytical ODS column with a linear gradient of methanol (from 2.5 to 80%) in 0.1% heptafluorobutylic acid (pH 3.0), and the UV/vis absorption spectrum of the ethanesulfonic acid-dC was measured with a photodiode array detector.

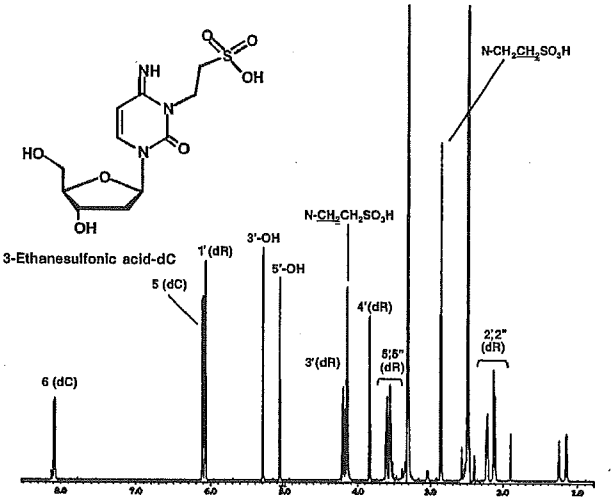

Figure 3. ^{1}H NMR spectrum in DMSO-d_6 and chemical structure of the ethanesulfonic acid-dC adduct.

of the cytidine moiety (see Supporting Information). Therefore, the structure of this compound was concluded to be 3-ethanesulfonic acid-dC (Figure 3).

Formation of CA-dC and -dA Adducts by NO-TCA. As mentioned above, the DNA adduct-containing taurine moiety was clearly formed by NO-TCA. Then, the formation of bile acid-DNA adduct was analyzed by the ^{32}P-postlabeling method, under the different condition from the case of 3-ethanesulfonic acid-dC adduct.

As shown in Figure 4, two major adduct spots (Figure 4A) were clearly detected on reaction of NO-TCA with calf thymus DNA. Levels of these adduct spots were estimated to be 3.40 ± 0.16 (Figure 4A, spot 1) and 1.69 ± 0.20 (Figure 4A, spot 2) per 10^8 nucleotides. In addition, one minor adduct spot (Figure 4A, spot 3) was also observed and the adduct level was almost 10 times lower than those of major spots.

To confirm the nucleotides involved in these adducts, this nitroso compound was incubated with 2′-deoxyribonucleotide 3′-monophosphates, and adduct formation was analyzed by the ^{32}P-postlabeling method under nuclease P1 conditions. As shown in Figure 4B, the major adduct

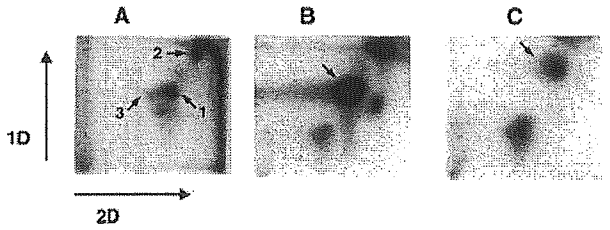

Figure 4. Autoradiograms of bile acid-DNA adducts derived from NO-TCA. NO-TCA was incubated with calf thymus DNA (A), 3′-dCp (B), and 3′-dAp (C) in 100 mM phosphate buffer (pH 7.4) at 37 °C for 24 h. Then adduct formations were analyzed by the ^{32}P-postlabeling method and developed with different conditions from the case of ethanesulfonic acid-dC adduct described in the Materials and Methods. Adducts are indicated by arrows.

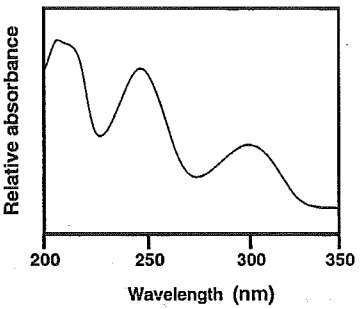

Figure 5. UV/vis absorption spectrum of the CA-dC adduct eluting at a retention time of 21.3 min on an ODS column and measured with a photodiode array detector.

spot (Figure 4A, spot 1) observed with the calf thymus DNA corresponded to the dC adduct, and another spot (Figure 4A, spot 2) corresponded to adduct spot detected in the reaction mixture of NO-TCA and 3′-dAp (Figure 4C). Moreover, the minor adduct spot (Figure 4A, spot 3) was deduced to be a dG adduct (data not shown). From these findings, DNA adducts detected in the NO-TCA treated calf thymus DNA were concluded to be NO-TCA-dC, NO-TCA-dA, and NO-TCA-dG. To analyze the chemical structure of the major adduct, NO-TCA was incubated with dC and the adduct was isolated by HPLC on an ODS column using a linear gradient of an acetonitrile in diethylamine-acetic acid (pH 6.0) solvent system. A peak eluting at a retention time of 21.3 min was observed in the reaction mixture of NO-TCA and dC. Thus, this peak fraction was collected and the UV/vis absorption spectrum of the responsible compound was measured. As shown in Figure 5, its absorption maxima were at 245 and 298 nm. Mass spectrometry demonstrated a molecular ion at *m/z* 618, which corresponded to a protonation product of a CA and deoxycytidine conjugate. A prominent fragment peak observed at *m/z* 502 was consistent with loss of the deoxyribose moiety from the protonated molecule. The authentic sample of N^4-cholyl-dC showed UV absorption maxima at 243 and 295 nm and exhibited a molecular ion of *m/z* 618. Therefore, the dC adduct formed from NO-TCA was deduced to be CA-dC adduct. By repeating the HPLC fractionation, about 400 μg of the CA-dC adduct could be collected for measurement of the ^{1}H NMR spectrum. The yield of CA-dC adduct from dC was about 0.06%. Figure 6A shows the ^{1}H NMR spectrum for the CA-dC adduct measured in DMSO-d_6, indicating the presence of 52 protons, which were assigned by two-dimensional NMR and comparison with NMR spectral data obtained from the authentic sample of N^4-cholyl-dC (Figure 6B). Forty upfield peaks from 0.57 to 4.27 ppm were assigned to the CA moiety. Proton signals corresponding to the 2′-deoxycytidine moiety [H-1′, 2′, 2″, 3′, 4′, 5′, 5″, 3′-OH, 5′-OH (dR), H-5, -6 (dC)] were also observed from 1.98 to 8.30 ppm. Thus, all proton signals of the product formed from NO-TCA and dC agreed with those of authentic N^4-cholyl-dC. Its structure is shown in Figure 7.

From the results of ^{32}P-postlabeling analysis, another major DNA adduct produced by NO-TCA with calf thymus DNA was suggested to contain a dA moiety. Speculating from the results of the dC adduct described above, the structure of the dA adduct derived from NO-TCA was suggested to be N^6-cholyl-dA. To confirm the structure of the NO-TCA-dA adduct, NO-TCA was incubated with dA in 100 mM phosphate buffer (pH 7.4) at 37 °C for 24 h and separated by HPLC under the same conditions for structural analysis of the CA-dC adduct. A peak eluting at a retention time of 15.4 min, the same as for authentic N^6-cholyl-dA, was observed in the reaction mixture. Moreover, this peak fraction had a similar UV absorption spectrum, with an absorption maximum at 273 nm, to that of the authentic sample of N^6-cholyl-dA (absorption maximum at 272 nm). LC-ESI/MS analysis revealed a molecular ion at *m/z* 642, corresponding to a protonated product of a CA and deoxyadenosine conjugate, and a fragmention ion at *m/z* 526, derived from the loss of the deoxyribose moiety from the original compound (Figure 8). From these observations, the chemical structure of this compound was concluded to be N^6-cholyl-2′-dA (Figure 8).

Structures of Adducts Formed by NO-TDCA. The other *N*-nitroso bile acid conjugate, NO-TDCA, would be expected to form similar dC adducts, including ethane sulfonic acid or deoxycholyc acid moiety. Therefore, NO-TDCA was incubated with dC, and the adduct formation was analyzed by LC-ESI/MS. A peak revealing a molecular ion at *m/z* 334 and its fragmentation ion at *m/z* 218 was eluted at the same retention time of 3-ethanesulfonic acid-dC (data not shown). Moreover, the UV/vis absorption pattern of this compound was identical to that of 3-ethanesulfonic acid-dC. Thus, 3-ethanesulfonic acid-dC was also produced from NO-TDCA and dC, and its yield was about the same levels as those of NO-TCA.

To confirm the formation of dC adduct including DCA moiety, NO-TDCA was incubated with dC and the adduct was isolated by HPLC on an ODS column according to the same procedures of N^4-cholyl-dC. The UV absorption pattern of this purified compound was similar to that of N^4-cholyl-dC, and its absorption maxima were at 246 and 298 nm (see Supporting Information). Like the N^4-cholyl-dC adduct, this compound exhibited a molecular ion at *m/z* 602, corresponding to a protonated product of DCA and dC conjugate, and a fragmentation ion at *m/z* 486, consistent with loss of the deoxyribose moiety from the protonated molecule (see Supporting Information). By repeating the HPLC procedures, around 1000 μg of the DCA-dC adduct could be collected for ^{1}H and ^{13}C NMR spectrum analysis. The yield of DCA-dC adduct from dC was 0.02%, and the ^{1}H and ^{13}C NMR spectra were assigned with DQF-COSY, HMQC, and HMBC (see Supporting Information). On the basis of the UV/vis, mass, and NMR spectral data, the structure of the adduct formed from NO-TDCA and dC was concluded to be N^4-deoxycholyl-dC (see Supporting Information).

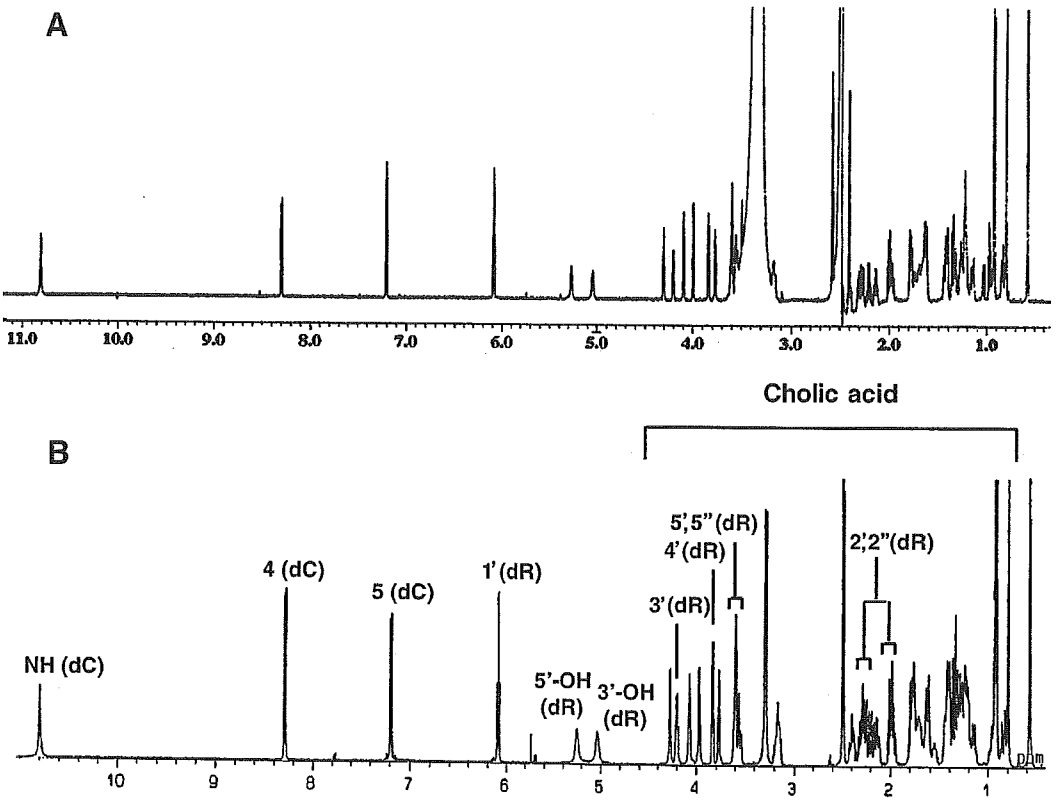

Figure 6. Comparison of the ^{1}H NMR spectra in DMSO-d_6 of CA-dC adduct (A) and authentic N^4-cholyl-dC (B).

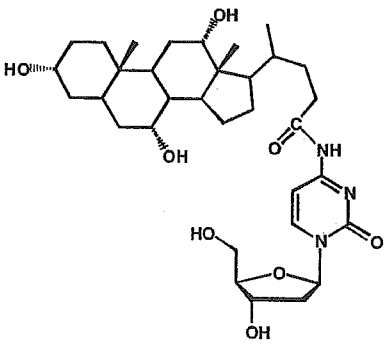

Figure 7. Chemical structure of N^4-cholyl-dC.

Mutagenic Activity of *N*-Nitroso Bile Acid Conjugates in *Salmonella* Strains. Mutagenic responses of *N*-nitroso bile acid conjugates in TA98 and TA100 were examined without metabolic activation. NO-TCA and NO-TDCA showed mutagenicity to TA100 in a dose-dependent manner but did not induce revertants in TA98. Their mutagenic activities were 9488 revertants for NO-TCA and 20800 revertants for NO-TDCA per μmol. Analysis of reverse mutations occurring at the *hisG46* site of TA100 with NO-TCA by DNA sequencing (Table 1) revealed G:C to A:T transitions dominantly. Among these, the pattern of CCC to CTC was almost four times higher than those of spontaneous mutations.

In Vivo Formation of Ethanesulfonic Acid-dC and N^4-Cholyl-dC. To confirm the formation of DNA adducts derived from bile acid conjugates in vivo, NO-TCA was singly injected at a dose of 250 mg/kg into Wistar rats by gavage, and then, 3-ethanesulfonic acid-dC and N^4-cholyl-dC were analyzed in the liver, glandular stomach, and colon mucosa, by a combination of HPLC separation and ^{32}P-postlabeling analysis. One hundred microgram aliquots of DNA digests were subjected to HPLC, and eluates were collected at 1 min intervals at retention times of 3−4 and 46−47 min, for the analysis of 3-ethanesulfonic acid-dC and N^4-cholyl-dC, respectively. The fractions were lyophilized and then analyzed by the ^{32}P-postlabeling method under nuclease P1 conditions. The adduct spot corresponding to the 3-ethanesulfonic acid-dC could be detected in the stomach and colon mucosa but not in the liver of rats treated with NO-TCA; no adduct spots were detected in these organs of control rats (Figure 9A). Adduct levels were estimated to be 0.22 ± 0.05 for stomach and 0.29 ± 0.09 for colon per 10^6 nucleotides. As the case of 3-ethanesulfonic acid-dC adduct, N^4-cholyl-dC adduct was seen in the stomach and colon mucosa of NO-TCA treated animals at estimated levels of 0.51 ± 0.33 and 0.67 ± 0.42 per 10^9 nucleotides, respectively (Figure 9B), although no adduct spot corresponding to N^4-cholyl-dC could be detected in fraction samples at a retention time of 46−47 min from control rats.

Discussion

The present study revealed formation and chemical structures of DNA adducts derived from *N*-nitroso bile acid conjugates using the ^{32}P-postlabeling method and various spectrometry techniques. Ethanesulfonic acid-dC adduct was formed from NO-TCA or NO-TDCA with calf thymus DNA or 2′-deoxynucleotides as a major adduct, and its chemical structure was concluded to be 3-ethanesulfonic acid-dC. In the case of reaction between NO-GCA with DNA, the major adducts were earlier demonstrated to be 7-carboxymethylguanine, 3-carboxymethyladenine,

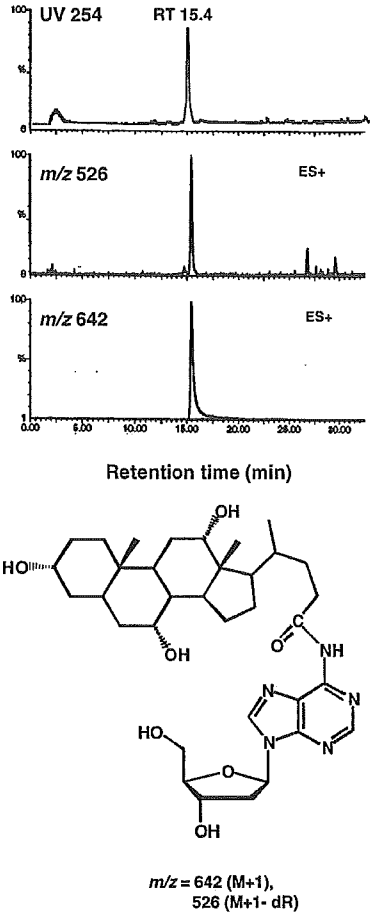

Figure 8. LC-ESI/MS analysis and chemical structure of the CA-dA adduct. An aliquot of purified CA-dA adduct was subjected on an analytical grade ODS column under the same conditions as used in CA-dC adduct and detected by UV (254 nm) absorption and ESI/MS (*m/z* 642 and 526, M + 1). Proposed mass of *m/z* = 642 corresponds to the $[M + H]^+$ of the N^6-cholyl-dA. A fragmentation at *m/z* 526 corresponded to the loss of the deoxyribose moiety from the original compound.

Table 1. Mutation Spectra for *hisG46* Reversions of TA100 Treated with NO-TCA

	TA100	
	control	NO-TCA
	G:C to A:T	
TCC (Ser)	11	11
CTC (Leu)	21	76
	G:C to T:A	
ACC (Thr)	37	13
CAC (His)	26	0
	G:C to C:G	
GCC (Ala)	5	0
%	100	100
no. of mutants	(19)	(53)

and O^6-carboxymethylguanine (*28*). As with formation of carboxymethyl-DNA adducts, ethanesulfonic acid adducts with other nucleotides than dC might be formed from NO-TCA and DNA. However, only a single spot could be detected in the reaction mixture of NO-TCA and 3′-dCp under the ^{32}P-postlabeling conditions used in the present study. On the other hand, several adducts containing a bile acid moieties were also formed from NO-TCA or NO-TDCA with calf thymus DNA or 2′-deoxyribonucleotides. The chemical structures of these major adducts were

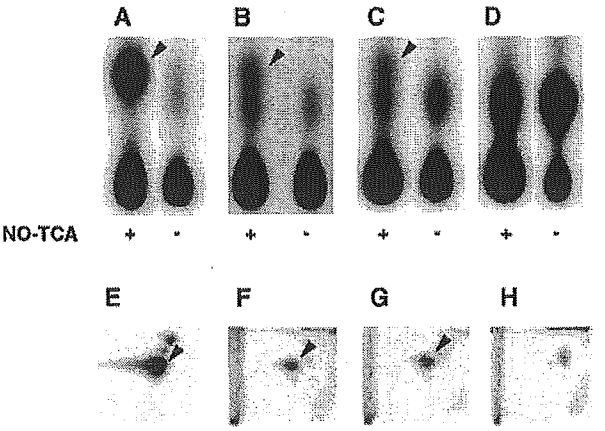

Figure 9. Autoradiograms of 3-ethanesulfonic acid-dC (A–D) and N^4-cholyl-dC (E–H) in calf thymus DNA or some organs of Wistar rats treated with or without NO-TCA. Adducts were analyzed by a combination of HPLC separation and ^{32}P-post-labeling analysis, as described in the Materials and Methods. Calf thymus DNA treated with NO-TCA (A, E) was used as a positive control. DNA samples were isolated from glandular stomach (B, F), colon mucosa (C, G), and liver (D, H) of rats with or without NO-TCA treatment. Adducts are indicated by the arrowheads.

concluded to be N^4-cholyl-dC, N^4-deoxycholyl-dC, and N^6-cholyl-dA, respectively, by spectrometry analysis. In addition, one minor adduct formed from NO-TCA and calf thymus DNA was suggested to be a dG adduct, although its chemical structure has yet to be clarified. Because the carbonyl moiety of CA was found to bind to N^4- or N^6-exocyclic amino groups of dC or dA in the present study, it is possible that the structure of CA-dG is N^2-cholyl-dG. In general, the positions of N7-, O6-dG, and N3-dA are preferentially attacked by alkylating agents, and 7-dG and 3-dA adducts are well-known to be unstable; thus, these adducts undergo spontaneous cleavage of the glycosidic bond, to produce abasic sites in DNA (*34*). Therefore, if 7-dG- or 3-dA-ethanesulfonic acid or bile acid adducts are produced from NO-TCA or NO-TDCA, they would be impossible to be detected by the ^{32}P-postlabeling methods used in the present study. As shown in Scheme 1, possible mechanisms for the formation of 3-ethanesulfonic acid-dC might be involved in the decomposition products of *N*-nitroso tauro bile acid conjugates. Dayal et al. have reported that *N*-nitroso bile acid conjugates decompose between pH 6 and pH 9 in aqueous buffered solutions, to generate several carcinogenic species, such as alkyl diazoate and its protonated form (*27*, *34*). Such electrophilic species might be implicated in the alkylation of DNA. In fact, the existence of electrophilic decomposition products of *N*-nitrosotauroursodeoxycholic acid, such as isethionic acid, diazoisethionic acid, and the protonated diazoate intermediate, has already been demonstrated by mass spectrum analysis (*27*). Meanwhile, there are no data regarding how bile acid-DNA adducts are formed at present; if the same mechanisms are involved in the generation of (deoxy)CA-DNA and ethanesulfonic acid-DNA, production of bile acid diazoate from NO-TCA or NO-TDCA would be necessary (Scheme 1). It has been well-known that the majority of the bulky-DNA adducts derived from exogenous mutagenic/carcinogenic compounds such as polycyclic aromatic hydrocarbons and heterocyclic amines have been identified as dG-C8 or dG-N2 adducts (*35*–*37*). However, in the present study, *N*-NO-bile acid conjugates preferentially

Scheme 1. Possible Reaction Mechanisms of *N*-Nitroso Bile Acid Conjugates and DNA

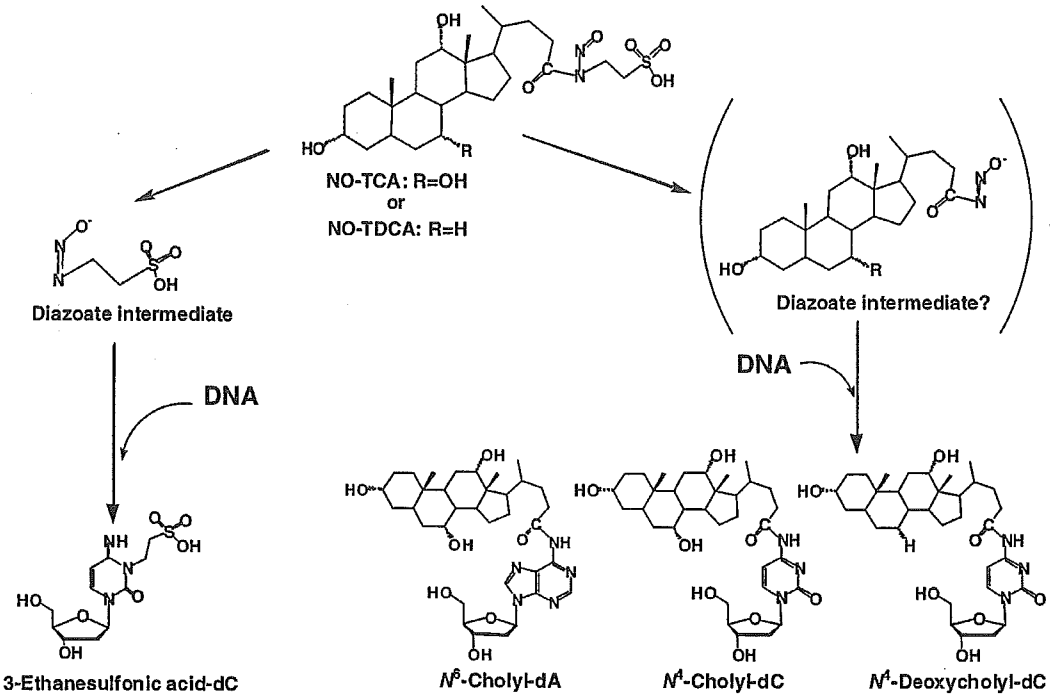

attacked the amino group at the N^4-position of dC and N^6-position of dA. Because the most reactive exocyclic amino group is known to be the N^4-position of dC, followed by the N^6-position of dA and the N^2-position of dG, it is likely that *N*-NO-bile acid conjugates could form N^4-cholyl-dC or N^6-cholyl-dA, rather than a dG adduct. Moreover, there are some reports describing the reaction between alkylating agents and cytidine or adenosine, and the N^3- and N^4-positions of dC and N^6-position of dA have been alkylated predominantly (*38*–*42*). In addition, the rearrangement of N^3-(deoxy)cholyl-dC or N^1-cholyl-dA to N^4-cholyl-dC or N^6-cholyl-dA is not ruled out. The mechanisms underlying formation of CA- or DCA-DNA adducts remain unclear. To understand the mechanisms for the formation of bile acid-DNA adducts, further study is needed.

Furthermore, we here demonstrated *N*-nitroso bile acid conjugates to induce mutations and their mutation spectrum in *S. typhimurium*. NO-TCA and NO-TDCA induced revertants to TA100, which detects base pair change mutations, but not in TA98, a detector of frameshift mutations. Moreover, NO-TCA induced G:C to A:T transitions predominantly in TA100, and most of them were CCC to CTC. This suggests that 3-ethanesulfonic acid- and N^4-cholyl-dC lead to G:C to A:T transitions. At present, there are no data to explain which adduct, ethanesulfonic acid- or CA-dC, is mainly responsible in TA100, and further studies are clearly warranted to clarify the mechanisms of mutagenicity.

When NO-TCA was injected to Wistar rats at a dose of 250 mg/kg, ethanesulfonic acid- and CA-DNA were detected in the glandular stomach and colon mucosa but not the liver, under the conditions used in the present study. While levels of these two kinds of adducts greatly differed, there was little variation between the two organ sites. Because the yield of CA-DNA in vitro was about 90 times lower than that of 3-ethanesulfonic acid-dC, it is reasonable that the yield of CA-DNA in vivo was also much lower than that of ethanesulfonic acid-DNA. Moreover, it has been reported that NO-TCA is not stable under physiological conditions and thus might easily produce the chemically active compound, alkyl diazoate, and inactive compounds, such as free bile acids (*27*). In the present study, NO-TCA was singly administered to rats by intragastric intubation and the stomach and colon mucosa would have been exposed to decomposition products. However, active compound apparently did not reach to the hepatic cells or only at very low levels. Alternatively, NO-TCA was efficiently inactivated by enzymes in the liver. It should be borne in mind that Busby et al. previously demonstrated NO-TCA to induce liver and stomach tumors in rats (*16*), with administration by gavage for 6 consecutive weeks with a total of 300 mg compound per rat. To clarify the tissue distribution of ethanesulfonic acid-dC and CA-DNA, an increase in the amount of NO-TCA and/or differing administration routes need to be explored.

Nitrosation of bile acid conjugates can be mediated by the acid-catalyzed reaction of amides with nitrite (*14*) and activated macrophages in infected and inflamed organs also believed to be involved in such reactions. Thus, nitrosated bile acid conjugates might contribute to human cancer development as endogenous mutagens. It is well-documented that G to A base substitutions are frequently observed in cancer related genes, such as *ras* family members and *p53* (*43*–*45*). Chemical instability might explain why nitroso bile acid derivatives have not been detected in any biological samples so far tested (*46*). Targeting specific DNA adducts, such as 3-ethanesulfonic acid-dC, N^4-cholyl-dC, N^4-deoxycholyl-dC, and N^6-cholyl-dA, therefore appears to be a useful way of monitoring endogenous formation of nitrosated bile acid conjugates. To clarify involvement of these nitroso bile acid conjugates in human carcinogenesis, it is clearly necessary to evaluate exposure levels.

Acknowledgment. This study was supported by Grants-in-Aid for Cancer Research from the Ministry of Health, Labor and Welfare of Japan and for scientific research from the Japan Society for the Promotion of Science. We acknowledge the contributions of Dr. T. Suzuki (Department of Biological Pharmacy School of Pharmacy, Shujitsu University) in useful discussions. S.E. is the recipient of a Research Resident fellowship from the Foundation of Promotion of Cancer Research.

Supporting Information Available: HMBC spectrum of ethanesulfonic acid-dC adduct and various spectral data of DCA-dC. This material is available free of charge via the Internet at http://pubs.acs.org.

References

(1) Debruyne, P. R., Bruyneel, E. A., Li, X., Zimber, A., Gespach, C., and Mareel, M. M. (2001) The role of bile acids in carcinogenesis. *Mutat. Res. 480–481*, 359–369.

(2) de Kok, T. M., and van Maanen, J. M. (2000) Evaluation of fecal mutagenicity and colorectal cancer risk. *Mutat. Res. 463*, 53–101.

(3) Owen, R. W. (1997) Faecal steroids and colorectal carcinogenesis. *Scand. J. Gastroenterol. 222* (Suppl.), 76–82.

(4) Kishida, T., Taguchi, F., Feng, L., Tatsuguchi, A., Sato, J., Fujimori, S., Tachikawa, H., Tamagawa, T., Yoshida, Y., and Kobayashi, M. (1997) Analysis of bile acids in colon residual liquid or fecal material in patients with cololectal neoplasia and control subjects. *J. Gastroenterol. 32*, 306–311.

(5) Deschner, E. E., Cohen, B. I., and Raicht, R. F. (1981) Acute and chronic effect of dietary cholic acids on colonic epithelial cell proliferation. *Digestion 21*, 290–296.

(6) Bartram, H. P., Scheppach, W., Schmid, H., Hofmann, A., Dusel, G., Richter, F., Richter, A., and Kasper, H. (1993) Proliferation of human colonic mucosa as an intermediate biomarker of carcinogenesis: Effects of butyrate, deoxycholate, calcium, ammonia, and pH. *Cancer Res. 53*, 3283–3288.

(7) Mcmillan, L., Butcher, S., Wallis, Y., Neoptolemos, J. P., and Lord, J. M. (2000) Bile acids reduce the apoptosis-inducing effects of sodium butyrate on human colon adenoma (AA/CC) cells: Implication for colon carcinogenesis. *Biochem. Biophys. Res. Commun. 273*, 45–49.

(8) Narisawa, T., Magadia, N. E., Weisburger, J. H., and Wynder, E. L. (1974) Promoting effect of bile acids on colon carcinogenesis after intrarectal instillation of *N*-methyl-*N'*-nitrosoguanidine in rats. *J. Natl. Cancer Inst. 53*, 1093–1097.

(9) Reddy, B. S., Watanabe, K., Weisburger, J. H., and Wynder, E. L. (1977) Promoting effect of bile acids in colon carcinogenesis in germ-free and conventional F344 rats. *Cancer Res. 37*, 3228–3242.

(10) Hamada, K., Umemoto, A., Kajikawa, A., Seraj, M. J., and Monden, Y. (1994) *In vitro* formation of DNA adducts with bile acids. *Carcinogenesis 15*, 1911–1915.

(11) Scates, D. K., Spigelman, A. D., and Venitt, S. (1994) Bile acids do not form adducts when incubated with DNA in vitro. *Carcinogenesis 15*, 2945–2948.

(12) Scates, D. K., Spigelman, A. D., and Venitt, S. (1995) Appearance of artifacts when using ^{32}P-postlabeling to investigate DNA adduct formation by bile acids in vitro: Lack of evidence for covalent binding. *Carcinogenesis 16*, 1489–1491.

(13) Scates, D. K., Spigelman, A. D., Phillips, R. K. S., and Venitt, S. (1997) The use of ^{32}P-postlabeling in studies of the nature and origin of DNA adducts formed by bile from patients with familial adenomatous polyposis and from normal patients. *Mutat. Res. 378*, 113–125.

(14) Shuker, D. E. G., Tannenbaum, S. R., and Wishnok, J. S. (1981) *N*-Nitroso bile acid conjugates. 1. Synthesis, chemical reactivity, and mutagenic activity. *J. Org. Chem., 46*, 2092–2096.

(15) Puju, S., Shuker, D. E. G., Bishop, W. W., Falchuk, K. R., Tannenbaum, S. R., and Thilly, W. G. (1982). Mutagenicity of *N*-nitroso bile acid conjugates in *Salmonella typhimurium* and diploid human lymphoblasts. *Cancer Res. 42*, 2601–2604.

(16) Busby, W. F., Shuker, D. E. G., Charley, G., Newberne, P. M., Tannenbaum, S. R., and Wogan, G. N. (1985) Carcinogenicity in rats of the nitrosated bile acid conjugates: *N*-Nitrosoglycocholic acid and *N*-nitrosotaurocholic acid. *Cancer Res. 45*, 1367–1371.

(17) Miwa, K., Hasegawa, H., Fujimura, T., Matsumoto, H., Miyata, R., Kosaka, T., Miyazaki, I., and Hattori, T. (1992) Duodenal reflux through the pylorus induces gastric adenocarcinoma in the rat. *Carcinogenesis 13*, 2313–2316.

(18) Miwa, K., Kinami, S., Miyazaki, I., and Hattori, T. (1996) Positive association between dietary fat intake and risk of gastric stump carcinoma in rats. *Carcinogenesis 17*, 1885–1889.

(19) Kumagai, H., Mukaisyo, K., Sugihara, H., Miwa, K., Yamamoto, G., and Hattori, T. (2004) Thioproline inhibits development of esophageal adenocarcinoma induced by gastroduodenal reflux in rats. *Carcinogenesis 25*, 723–727.

(20) Caygill, C. P., Hill, M. J., Kirkham, J. S., and Northfield, T. C. (1986) Mortality from gastric cancer following gastric surgery for peptic ulcer. *Lancet 1*, 929–931.

(21) Viste, A., Bjornestad, E., Opheim, P., Skarstein, A., Thunold, J., Hartveit, F., Eide, G. E., Eide, T. J., and Soreide, O. (1986) Risk of carcinoma following gastric operations for benign disease: A historical cohort study of 3470 patients. *Lancet 2*, 502–504.

(22) Lundegardh, G., Adami, H. O., Helmick, C., Zack, M., and Meirik, O. (1988) Stomach cancer after partial gastrectomy for benign ulcer disease. *N. Engl. J. Med. 319*, 195–200.

(23) Toftgaard, C. (1989) Gastric cancer after peptic ulcer surgery. A historic prospective cohort investigation. *Ann. Surg. 210*, 159–164.

(24) Street J. M., Trafford, D. J. H., and Makin H. L. J. (1983) The quantitative estimation of bile acids and their conjugates in human biological fluids. *J. Lipid Res. 24*, 491–511.

(25) Scalia, S. (1988) Simultaneous determination of free and conjugated bile acids in human gastric juice by high-performance liquid chromatography. *J. Chromatogr. 431*, 259–269.

(26) Mirvish, S. S. (1995) Role of *N*-nitroso compounds (NOC) and *N*-nitrosation in etiology of gastric, esophageal, nasopharyngeal and bladder cancer and contribution to cancer of known exposures to NOC. *Cancer Lett. 93*, 17–48.

(27) Dayal, B., and Ertel, N. H. (1997) Studies on *N*-nitroso bile acid amides in relation to their possible role in gastrointestinal cancer. *Lipids 32*, 1331–1340.

(28) Shuker, D. E. G., and Margison, G. P. (1997) Nitrosated glycine derivatives as a potential source of O^6-methylguanine in DNA. *Cancer Res. 57*, 366–369.

(29) Takamura, T., Sugimura, T., and Wakabayashi, K. (2004) Formation of DNA adducts by reactive intermediates, bile acid-adenylate. Proceedings of 63rd Annual Meeting of the Japanese Cancer Association, p 85.

(30) Reddy, M. V., and Randerath, K. (1986) Nuclease P1-mediated enhancement of sensitivity of ^{32}P-postlabeling test for structurally diverse DNA adducts. *Carcinogenesis 7*, 1543–1551.

(31) Takamura-Enya, T., Watanabe, M., Totsuka, Y., Kanazawa, T., Matsushima-Hibiya, Y., Koyama, K., Sugimura, T., and Wakabayashi, K. (2001) Mono(ADP-ribosyl)ation of 2′-deoxyguanosine residue in DNA by an apoptosis-inducing protein, pierisin-1, from cabbage butterfly. *Proc. Natl. Acad. Sci. U.S.A. 98*, 12414–12419.

(32) Gupta, R. C. (1985) Enhanced sensitivity of ^{32}P-post-labeling analysis of aromatic carcinogen: DNA adducts. *Cancer Res. 45*, 5656–5662.

(33) Yahagi, T., Nagao, M., Seino, Y., Matsushima, T., Sugimuta, T., and Okada, M. (1977) Mutagenicities of *N*-nitrosoamines on *Salmonella*. *Mutat. Res. 48*, 121–130.

(34) Dayal, B., Bhojawala, J., Rapole, K. R., Pramanik, B. N., Ertel, N. H., Shefer, S., and Salen, G. (1996) Chemical synthesis, structural analysis, and decomposition of *N*-nitroso bile acid conjugates. *Bioorg. Med. Chem. 4*, 885–890.

(35) Chen, S. C., Hilton, B. D., Roman, J. M., and Dipple, A. (1989) DNA adducts from carcinogenic and noncarcinogenic enantiomers of benzo[*a*]pyrene dihydrodiol epoxide. *Chem. Res. Toxicol. 2*, 334–340.

(36) Sayer, J. M., Chadha, A., Agarwal, H. S. K., Yeh, H. J. C., Yagi, H., and Jerina, D. M. (1991) Covalent nucleoside adducts of benzo[*a*]pyrene 7,8-diol 9,10-epoxides: Structural reinvestigation and characterization of a novel adenosine adduct on the ribose moiety. *J. Org. Chem. 56*, 20–29.

(37) Snyderwine, E. G., and Turteltaub, K. W. (2000) Interactions with cellular macromolecules. In *Food Borne Carcinogenic Heterocyclic Amines* (Nagao, M., and Sugimura, T., Eds.) pp 131–161, John Wiley & Sons Ltd., West Sussex.

(38) Brookes, P., and Lawley, P. D. (1962) The methylation of cytosine and cytidine. *J. Chem. Soc.* 1348.

(39) Sun, L., and Singer, B. (1974) Reaction of cytidine with ethylating agents. *Biochemistry 13*, 1905–1913.

(40) Singer, B., Sun, L., and Fraenkel-Conrat, H. (1974) Reaction of adenosine with ethylating agents. *Biochemistry 13*, 1913–1920.

(41) Singer, B. (1976) O^2-Alkylcytidine—A new major product of neutral, aqueous reaction of cytidine with carcinogens. *FEBS Lett. 63*, 85−88.
(42) Segal, A., Solomon, J. J., Mignano, J., and Dino, J. (1981) The isolation and characterization of 3-(2-carboxyethyl)cytosine following in vitro reaction of b-propiolactone with calf thymus DNA. *Chem. Biol. Interact. 35*, 349−361.
(43) Smith, G., Crey, F. A., Beattie, J., Wilkie, M. J., Lightfoot, T. J., Coxhead, J., Garner, R. C., Steele, R. J. C., and Wolf, R. (2002) Mutations in APC, Kirsten-ras, and p53-alternative genetic pathways to colorectal cancer. *Proc. Natl. Acad. Sci. U.S.A. 99*, 9433−9438.
(44) Gealy, R., Zhang, L., Siegfried, J. M., Luketich, J. D., and Keohavong, P. (1999) Comparison of mutations in the p53 and K-ras genes in lung carcinomas from smoking and nonsmoking women. *Cancer Epidemiol., Biomarkers Prev. 8*, 297−302.
(45) Olivier, M., Hussain, S. P., de Fromentel, C. C., Hainaut, P., and Harris, C. C. (2004) TP53 mutation spectra and load: A tool for generating hypotheses on the etiology of cancer. In *Mechanisms of Carcinogenesis: Contributions of Molecular Epidemiology* (Buffler, P., Rice, J., Baan, R., Bird, M., and Boffetta, P., Eds.) IARC Scientific Publications No. 157, pp 247−270, IARC, Lyon.
(46) Fein, M., Fuchs, K.-H., Stopper, H., Diem, S., and Herderich, M. (2000) Duodenogastric reflux and foregut carcinogenesis: Analysis of duodenal juice in a rodent model of cancer. *Carcinogenesis 21*, 2079−2083.

TX050144X

Environmental and Molecular Mutagenesis 47:48–55 (2006)

MX, a By-Product of Water Chlorination, Lacks In Vivo Genotoxicity in *gpt* Delta Mice but Inhibits Gap Junctional Intercellular Communication in Rat WB Cells

Akiyoshi Nishikawa,[1]* Kimie Sai,[2] Kazushi Okazaki,[1] Hwa-Young Son,[1] Keita Kanki,[1] Madoka Nakajima,[3] Naohide Kinae,[3] Takehiko Nohmi,[4] James E. Trosko,[5] Tohru Inoue,[6] and Masao Hirose[1]

[1]*Division of Pathology, National Institute of Health Sciences, Tokyo 158-8501, Japan*
[2]*Division of Biosignaling, National Institute of Health Sciences, Tokyo 158-8501, Japan*
[3]*Laboratory of Food Hygiene, School of Food and Nutritional Science, University of Shizuoka, Shizuoka 422-8526, Japan*
[4]*Division of Genetics and Mutagenesis, National Institute of Health Sciences, Tokyo 158-8501, Japan*
[5]*National Food Safety Toxicology Center, Department of Pediatrics and Human Development, Michigan State University, East Lansing, MI 48824, U.S.A.*
[6]*Division of the Biological Safety Research Center, National Institute of Health Sciences, Tokyo 158-8501, Japan*

3-Chloro-4-(dichloromethyl)−5-hydroxy-2(*5H*)-furanone (MX), a by-product of water chlorination, is a potent bacterial mutagen and rat carcinogen. In the present study, the in vivo mutagenicity, cell proliferative activity, and carcinogenicity of MX were investigated in *gpt* delta mice. Groups of 5 male and female 7-week-old *gpt* delta C57BL/6J transgenic mice were given MX at doses of 0, 10, 30, or 100 ppm in their drinking water for 12 weeks, and then killed to assess in vivo mutagenicity using 6-thioguanine and Spi$^-$ selection, and cell proliferative activity using immunohistochemistry for proliferating cell nuclear antigen (PCNA). Further groups of 10 male and female *gpt* delta mice were given 0 or 100 ppm MX for 78 weeks, and a full necropsy with histopathological examination of all organs was conducted to detect neoplastic lesions. The 12-week MX treatment did not result in mutagenicity in the livers or lungs or cell proliferative activity in several organs of the mice, and the 78-week treatment did not cause carcinogenicity. Additional investigations were conducted to evaluate the potential of MX to inhibit gap junctional intercellular communication (GJIC) in rat liver epithelial cells (WB cells) by the scrape loading/dye transfer method. Inhibition of GJIC was detected within 2 hr with a noncytotoxic dose of MX (4 μg/ml), followed by partial restoration after 5 hr. A second phase of inhibition occurred after 10 hr and then the lowered level persisted for the 24 hr-incubation period. Dose-dependent inhibition was evident at both 2 hr and 24 hr, with much stronger effects at the former time. These findings indicate that MX is not mutagenic, mitogenic or carcinogenic in mice, and suggest that the compound exerts epigenetic actions leading to GJIC inhibition. Environ. Mol. Mutagen. 47:48–55, 2006.

Key words: MX; in vivo genotoxicity; gap junction

INTRODUCTION

3-Chloro-4-(dichloromethyl)−5-hydroxy-2(*5H*)-furanone (MX) (illustrated in Fig. 1), a by-product resulting from organic acid reactions during chlorine disinfection, has been isolated and identified as a nonvolatile compound in drinking water from several countries, including Finland [Hemming et al., 1986], the United States [Meier et al., 1987 a,b], England [Horth et al., 1989], and Japan [Suzuki and Nakanishi, 1990]. MX is strongly mutagenic in *Salmonella typhimurium* without metabolic activation

This article contains supplementary material available via the Internet at http:www.interscience.wiley.com/jpages/0893-6692/suppmat.

*Correspondence to: Akiyoshi Nishikawa, Division of Pathology, National Institute of Health Sciences, 1-18-1 Kamiyoga, Setagaya-ku, Tokyo 158-8501, Japan. E-mail: nishikaw@nihs.go.jp

Received 27 April 2005; provisionally accepted 12 May 2005; and in final form 10 June 2005

DOI 10.1002/em.20167

Published online 16 August 2005 in Wiley InterScience (www.interscience.wiley.com).

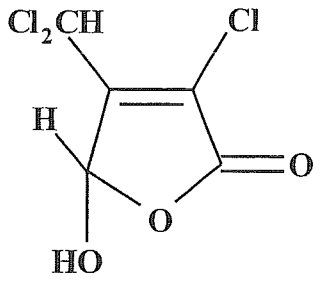

Fig. 1. Structure of MX.

[Ishiguro et al., 1988], and a Finnish group demonstrated the carcinogenicity of MX in the liver, thyroid gland, and lung of rats [Komulainen et al., 1997]. In addition, it has been reported that MX enhances replicative DNA synthesis and increases ornithine decarboxylase activity in the glandular stomach of rats when administered by gastric intubation at extremely high doses (10–60 mg/kg body weight) [Furihata et al., 1992]. We also have demonstrated that MX stimulates cell proliferation in the rat gastric mucosa [Nishikawa et al., 1994] and promotes glandular stomach carcinogenesis in rats pretreated with *N*-methyl-*N'*-nitro-*N*-nitrosoguanidine (MNNG) [Nishikawa et al., 1999].

Transgenic rodents are useful tools for assessing the in vivo mutagenicity of environmental mutagens [Gorelick and Mirsalis, 1996; Nohmi et al., 2000]. Their use permits the efficient and quantitative detection of mutations in any tissue of rodents, and it is possible to examine the correlation between mutagenicity and carcinogenicity at the organ levels. *Gpt* delta transgenic mice were established to increase the range of mutations detected by transgenic mutagenicity assays [Nohmi et al., 1996]. The *gpt* system detects point mutations in the *E. coli gpt* reporter gene by 6-thioguanine selection, as well as deletions with sizes of more than 1 kb by Spi^- selection [Nohmi et al., 1999; Horiguchi et al., 2001; Masumura et al., 2002; Takeiri et al., 2003].

Gap junctions have been linked to apoptotic processes [Trosko and Goodman, 1994; Wilson et al., 2000], as well as to tumor promotion [Trosko et al., 1983]. The transfer of ions and small molecular weight molecules is mediated through gap junctions, which are composed of two juxtaposed connections consisting of a hexamer of proteins, the connexins [Loewenstein, 1979; Evans and Martin, 2002]. Tumor promoting chemicals, by disrupting gap junctional intercellular communication (GJIC), have been postulated to isolate transformed cells from regulation, suppressing cell growth by surrounding normal cells [Yotti et al., 1979], and thus permitting their clonal expansion. Activated oncogenes, growth factors, and hormones that act as tumor-promoters also can down-regulate GJIC [Trosko and Ruch, 1998]. Several tumor-promoters such as phenobarbital, phorbol esters, and peroxisome proliferators inhibit GJIC [Trosko and Chang, 1988] and, conversely, anti-tumor promoting chemicals such as retinoids and dexamethasone can enhance GJIC [Grassilli et al., 1992; Trosko and Ruch, 2003]. These observations suggest a mechanistic association between tumor promotion and GJIC inhibition.

To cast light on the molecular mechanisms underlying the tumorigenic action of MX, its tumor-initiating potential was examined with reference to in vivo mutagenicity, cell proliferative activity, and carcinogenicity in *gpt* delta transgenic mice. In addition, its effect on GJIC was examined in rat liver epithelial cells by the scrape loading/dye transfer method.

MATERIALS AND METHODS

Synthesis of MX

MX was synthesized from tetrachloroacetone and (carbomethoxymethylene)-triphenylphosphorane, according to the method of Padmapria et al. [1985]. It was determined to be >97% pure, by high-performance liquid chromatography (R-ODS-5 column; YMS, Osaka, Japan).

Bioassay

Groups of five male and female 7-week-old *gpt* delta C57BL/6J transgenic mice were given MX at doses of 10, 30, or 100 ppm in their drinking water for 12 weeks. The highest dose was selected because 100 ppm is 10^6-fold the prevalent environmental level [Hemming et al., 1986; Meier et al., 1987; Horth et al., 1989; Suzuki and Nakanishi, 1990; Kinae et al., 1992], and nearly 1.5-fold higher than the highest concentration used in a previous rat carcinogenicity study [Komulainen et al., 1997]. On the basis of our previous study in which MX was rather stable at pH 7 and >70% remained in the drinking water after 2 days [Kinae et al., 1992], the drinking water was renewed every other day. Further groups of 10 male and female *gpt* delta mice were given 100 ppm MX for 78 weeks. The controls received tap water throughout the experiment.

After the treatment period of 12 weeks in the first experiment, mice were killed to assess cell proliferative activity by proliferating cell nuclear antigen (PCNA) immunohistochemistry, with the calculation of labeling indices as described previously [Nishikawa et al., 1994]. In the 78-week study, surviving animals were fully necropsied and all the organs were examined histopathologically for neoplastic lesions.

Rescue of Phages

Genomic DNAs were extracted from the liver and lung by phenol/chloroform extraction as previously described [Nohmi et al., 2000]. Briefly, the tissue samples were homogenized with a Dounce homogenizer, and the nuclei were collected by centrifugation. The resuspended nuclei were treated with SDS and proteinase K at 50°C for 1–2 hr, and the digests were extracted with equal volumes of phenol/chloroform and chloroform. DNA was precipitated with ethanol, washed with 70% ethanol, and dissolved in TE-4 buffer. Lambda EG10 phages were rescued from genomic DNA by an in vitro packaging method, using Transpack™ packaging extract (Stratagene, La Jolla, CA).

Gpt Mutation Assay

The *gpt* mutation assay was performed as described previously [Nohmi et al., 2000]. Briefly, the rescued phages were infected into *E. coli* YG6020 expressing Cre recombinase to convert the transgene into a

TABLE I. Body Weight and Relative Organ Weights for Mice Treated Orally with MX for 12 Weeks

Treatment	No. of mice	Body weight (g)	Liver (%)	Kidneys (%)	Lungs (%)	Spleen (%)	Testes (%)
Male							
Control	5	31.8 ± 2.7[a]	4.39 ± 0.43	1.09 ± 0.13	0.24 ± 0.02	0.21 ± 0.04	0.66 ± 0.05
MX 10 ppm	5	30.7 ± 1.7	4.25 ± 0.35	1.15 ± 0.10	0.25 ± 0.02	0.25 ± 0.04	0.67 ± 0.05
MX 30 ppm	5	31.3 ± 2.4	4.44 ± 0.18	1.09 ± 0.05	0.25 ± 0.02	0.20 ± 0.02	0.70 ± 0.08
MX 100 ppm	5	29.8 ± 2.6	4.21 ± 0.33	1.07 ± 0.04	0.25 ± 0.03	0.22 ± 0.03	0.69 ± 0.05
Female							
Control	5	21.8 ± 0.8	4.24 ± 0.13	1.10 ± 0.09	0.29 ± 0.02	0.30 ± 0.06	
MX 10 ppm	5	21.5 ± 0.5	4.13 ± 0.12	1.10 ± 0.06	0.29 ± 0.02	0.32 ± 0.03	
MX 30 ppm	5	22.5 ± 1.1	4.27 ± 0.33	1.09 ± 0.05	0.29 ± 0.03	0.32 ± 0.03	
MX 100 ppm	5	22.6 ± 1.5	4.06 ± 0.09	1.07 ± 0.04	0.30 ± 0.03	0.32 ± 0.07	

[a]Data represent means ± SD.

plasmid. Infected cells were mixed with molten soft agar and poured onto agar plates containing chloramphenicol (Cm) and 6-thioguanine (6-TG). The plates were incubated at 37°C for the selection of colonies harboring plasmids carrying the chloramphenicol acetyltransferase gene and a mutated *gpt* gene. The rescued phages were also infected into YG6020, and poured on plates containing Cm without 6-TG to determine the number of rescued plasmids. The mutant frequency (MF) was calculated as described previously [Nohmi et al., 2000].

Spi⁻ Selection

Spi⁻ selection was performed as described previously [Nohmi et al., 2000]. Briefly, the packaged phages were incubated with *E. coli* XL-1 Blue MRA for survival titration and *E. coli* XL-1 Blue MRA P2 for mutant selection, respectively. Infected cells were mixed with molten lambda-trypticase soft agar and poured onto lambda-trypticase agar plates. On the following day, plaques (Spi⁻ candidates) were punched out using sterilized glass pipettes and suspended in SM buffer. To confirm the Spi⁻ phenotype of candidate mutant plaques, suspensions were spotted on three types of plates, with XL-1 Blue MRA, XL-1 Blue MRA P2, and WL95 P2 strains spread with soft agar. Confirmed Spi⁻ mutants making clear plaques on every strain were collected and stored as lysed phages at 4°C [Nohmi et al., 1999].

Cell Culture and Treatment with MX

MX was dissolved in 100% ethanol at a dose of 10 mg/ml and kept as a stock solution at −20°C until use. The stock solution was diluted in D-medium (Formula No. 78-5470EF, GIBCO, Grand Island, NY) without serum for treatment. WB-F344 rat liver epithelial cells (WB cells) of oval cell origin [Tsao et al., 1984] were obtained from Drs. J. W. Grisham and M. S. Tsao of the University of North Carolina (Chapel Hill, NC) and plated onto 35-mm dishes in 2 ml of D-medium, supplemented with 5% fetal bovine serum (GIBCO) at 37°C in a humidified atmosphere containing 5% CO_2 and 95% air. Confluent cells were washed with phosphate-buffered saline (PBS) and incubated with serum-free D-medium containing MX for up to 24 hr.

GJIC Assay

Before GJIC assay, the noncytotoxic range of MX was determined spectrophotometrically by measuring the absorbance of neutral red (Wako Chemical, Osaka, Japan) taken up into the cells at a wavelength of 540 nm, according to the method of Borenfeund and Puerna [1985]. The WB cells were treated with MX at concentrations ranging from 0.03 to 10 μg/ml for 24 hr, and viability was expressed as a fraction of the control value. GJIC was assessed in the noncytotoxic range of MX (0–4 μg/ml) by the scrape-loading and dye transfer method originally described by El-Fouly et al. [1987] with the slight modifications described in a previous report [Sai et al., 1998]. Briefly, after treatment with MX, the cells were washed with PBS and 0.05% Lucifer Yellow (LY) (Molecular Probes, Eugene, OR), and a fluorescent dye, which travels through gap junctions, dissolved in PBS, was added to the culture dish. For loading LY into cells, incisions were made on the cell monolayer by scraping with a blade. After incubation at room temperature for 3 min, the cells were washed with PBS and then fixed with 4% formalin. The distance of LY-transfer was viewed with a confocal microscope (Fluoview; Olympus, Tokyo, Japan) and measured by an analytical program in Fluoview. The value for GJIC was expressed as a fraction of the control value, as described previously [Sai et al., 1998].

Statistical Analysis

Data were evaluated by the Student's t-test or analysis of variance (ANOVA) followed by the Dunnett's multiple comparison test or the Kruskal-Wallis test.

RESULTS

Lack of Mutagenicity, Cell Proliferative Activity or Carcinogenicity

No *gpt* delta mice died during the 12-week treatment. There were no differences in water consumption (data not shown) or in body or organ weights between the groups, in either male or female mice, killed at 12 weeks (Table I). PCNA-labeling indices for various organs, including the liver, lung, kidney, and thyroid did not differ among the groups (data not shown), nor did they differ in the gastrointestinal tract (Table II). As shown in Table III, the MFs for the *gpt* gene in the livers and lungs of male mice were, respectively, 2.17, 2.32, 1.76 and 1.50 ($\times 10^{-6}$), and 1.88, 2.50, 1.82 and 2.05 ($\times 10^{-6}$) in the groups receiving 0, 10, 30, and 100 ppm MX for 12 weeks. The respective MFs in the livers of female mice were 2.03, 2.17, 4.19 and 2.40 ($\times 10^{-6}$) (Table III). As shown in Table IV, the MFs for the *red/gam* genes assessed by Spi⁻ selection in male livers and lungs were, respectively, 1.55, 1.74, 1.99 and 1.68, and 1.10, 0.84, 0.81 and 1.25 ($\times 10^{-6}$) in the groups treated with 0, 10,

TABLE II. PCNA-Labeling Indices (%) for the Gastrointestinal Tract of Mice Treated Orally with MX for 12 Weeks

Treatment	No. of mice	Fore-stomach	Glandular stomach	Duodenum	Jejunum	Ileum	Cecum	Colon	Rectum
Male									
Control	5	46.1 ± 5.3[a]	32.0 ± 2.5	42.1 ± 2.6	44.1 ± 4.2	43.2 ± 2.5	41.0 ± 2.8	36.3 ± 6.0	42.8 ± 2.0
MX 10 ppm	5	46.0 ± 3.0	32.9 ± 3.9	43.8 ± 4.9	45.0 ± 3.3	44.9 ± 4.0	39.5 ± 2.1	38.2 ± 3.6	39.1 ± 6.1
MX 30 ppm	5	48.6 ± 3.5	33.5 ± 2.9	44.2 ± 5.1	44.6 ± 3.3	42.1 ± 2.2	40.7 ± 1.4	37.7 ± 4.2	40.1 ± 3.1
MX 100 ppm	5	47.9 ± 3.1	33.6 ± 1.6	43.9 ± 3.6	45.7 ± 5.1	45.0 ± 4.0	39.2 ± 3.8	36.2 ± 2.5	38.3 ± 5.1
Female									
Control	5	43.5 ± 4.2	34.5 ± 5.0	44.4 ± 7.1	45.5 ± 4.6	41.0 ± 3.7	42.0 ± 3.5	33.4 ± 3.6	38.9 ± 4.3
MX 10 ppm	5	42.1 ± 2.9	33.6 ± 5.0	43.8 ± 4.7	43.9 ± 3.7	41.0 ± 4.6	41.9 ± 2.8	34.4 ± 4.1	36.9 ± 2.9
MX 30 ppm	5	43.6 ± 4.8	32.5 ± 3.6	44.9 ± 3.9	43.7 ± 2.3	44.2 ± 5.6	41.0 ± 2.8	35.6 ± 5.1	37.9 ± 3.7
MX 100 ppm	5	44.0 ± 3.3	33.4 ± 4.1	44.5 ± 4.5	44.5 ± 3.5	43.4 ± 3.5	40.7 ± 1.7	35.0 ± 5.0	39.5 ± 4.1

[a]Data represent means ± SD.

TABLE III. *Gpt* Mutant Frequency (MF) in Livers and Lungs of Mice Treated Orally with MX for 12 Weeks[a]

Treatment	No. of animals	No. of mutations	No. of colonies screened	MF ($\times 10^{-6}$)
Liver (Male)				
Control	5	7	3,675,000	2.17 ± 1.43[b]
MX 10 ppm	5	10	4,396,500	2.32 ± 1.61
MX 30 ppm	5	6	3,472,500	1.76 ± 2.46
MX 100 ppm	5	8	5,811,000	1.50 ± 0.97
Liver (Female)				
Control	5	7	3,159,000	2.03 ± 1.87
MX 10 ppm	5	4	2,191,500	2.17 ± 3.02
MX 30 ppm	5	9	2,479,500	4.19 ± 3.13
MX 100 ppm	5	6	2,239,500	2.40 ± 2.65
Lung (Male)				
Control	5	6	3,027,000	1.88 ± 1.48
MX 10 ppm	5	10	3,907,500	2.50 ± 1.76
MX 30 ppm	5	9	4,510,500	1.82 ± 1.19
MX 100 ppm	5	8	4,051,500	2.05 ± 1.43

[a]See web-based Supplementary Material for animal-by-animal data.
[b]Data represent means ± SD.

TABLE IV. Spi$^-$ Mutant Frequency (MF) in Livers and Lungs of Male Mice Treated Orally with MX for 12 Weeks[a]

Treatment	No. of animals	No. of mutations	No. of plaques screened	MF ($\times 10^{-6}$)
Liver				
Control	5	11	6,645,000	1.55 ± 1.24[b]
MX 10 ppm	5	16	9,267,000	1.74 ± 0.94
MX 30 ppm	5	17	9,774,000	1.99 ± 1.10
MX 100 ppm	5	17	10,245,000	1.68 ± 0.77
Lung				
Control	5	6	4,617,000	1.10 ± 0.80
MX 10 ppm	5	3	2,202,000	0.84 ± 1.11
MX 30 ppm	5	3	5,154,000	0.81 ± 1.14
MX 100 ppm	5	6	4,926,000	1.25 ± 1.27

[a]See web-based Supplementary Material for animal-by-animal data.
[b]Data represent means ± SD.

30 and 100 ppm MX for 12 weeks. Thus there were no differences in MFs between groups following the 12-week MX treatment. Similarly, the MFs for the *gpt* genes in nontumorous livers receiving 100 ppm MX for 78 weeks were comparable with those in corresponding control livers, in both male and female mice (Table V).

Although 2 out of 10 control males and 3 of 10 100-ppm MX-treated females were killed in a moribund condition or found dead before 78 weeks, four of these mice survived more than 52 weeks. Including these animals, only four neoplastic lesions were detected in total: lymphomas in one each of the treated and control males, and one histiocytic sarcoma, and one osteosarcoma in treated females. Thus, there was no evidence that MX was carcinogenic in this preliminary carcinogenicity study in which 10 male and female mice per group were tested.

Inhibition of GJIC

To select appropriate doses of MX for the GJIC assay (noncytotoxic range), cell viability was determined after MX-treatment. As shown in Figure 2, the highest dose of 10 μg/ml significantly ($P < 0.001$) reduced the viability of WB cells after MX treatment for 24 hr, and the second highest dose of 5 μg/ml produced a small reduction in viability. On the basis of this result, the maximum dose of MX was set to 4 μg/ml. After treatment of WB cells with a noncytotoxic dose of MX (4 μg/ml), GJIC was significantly ($P < 0.05$-0.001) inhibited throughout the 24 hr period (Fig. 3). Especially, marked inhibition of GJIC was observed within 2 hr, followed by a partial restoration after 5 hr (Fig. 4). A second phase of inhibition occurred at 10 hr and a slightly lower level of inhibition was detected in the 24-hr incubation sample (Fig. 4). A clear dose-dependent inhibition of GJIC in WB cells treated with MX at doses of 1, 2, and 4 μg/ml was observed for both the 2-hr and 24-hr incubations, with much stronger inhibition at 2 hr (Fig. 5).

DISCUSSION

In a previous carcinogenicity study using rats, MX induced tumors when given in drinking water at doses of 5.9–70.0 ppm for 104 weeks, with evidence of statistically significant increases of intrahepatic cholangiomas, lung

TABLE V. *Gpt* Mutant Frequency (MF) in Livers of Mice Treated Orally with 100 ppm MX for 78 Weeks[a]

Treatment	No. of animals	No. of mutations	No. of colonies screened	MF ($\times 10^{-6}$)
Male				
Control	5	8	2,068,500	3.35 ± 2.29[b]
100 ppm MX	5	16	4,302,000	3.63 ± 1.13
Female				
Control	5	7	3,205,500	2.47 ± 1.46
100 ppm MX	5	11	3,901,500	2.65 ± 2.16

[a]See web-based Supplementary Material for animal-by-animal data.
[b]Data represent means ± SD.

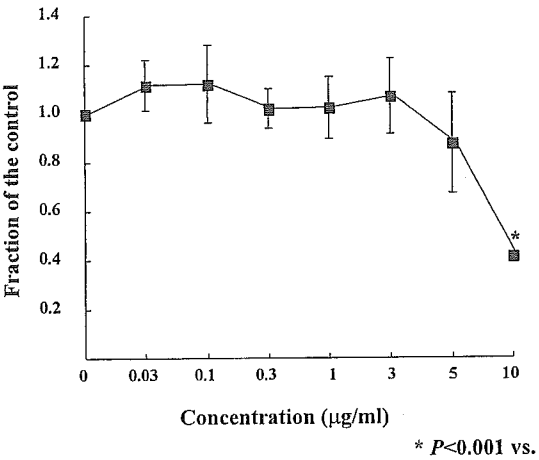

Fig. 2. Viability of WB cells after MX-treatment for 24 hr. Values are means ± SD from data of assays performed in triplicate.

adenomas, and some other tumors [Komulainen et al., 1997]. In the present study, however, MX, a strong in vitro mutagen, failed to exert in vivo mutagenicity or carcinogenicity in *gpt* delta mice. These results are consistent with a recent report of negative mutagenicity in *cII* transgenic medaka [Geter et al., 2004]. Our data provide additional information for assessing the human risk of MX because the species used, genes analyzed, and neoplastic lesions examined are more appropriate than those of the fish model. Transgenic medaka are possible resources for assessing ecological risks [Muir and Howard, 1999], but transgenic rodents have been shown to be more useful for assessing human risks of environmental chemicals [Gorelick and Mirsalis, 1996; Nohmi et al., 1996; Nohmi et al., 1999 ; Nohmi et al., 2000; Horiguchi et al., 2001; Masumura et al., 2002; Takeiri et al., 2003]. In addition, among reporter gene-transgenic rodent models, *gpt* delta mice and rats have an advantage in that not only point mutations but also deletions can be detected [Nohmi et al., 1996; Nohmi et al., 1999; Nohmi et al., 2000]. In the present study, the lack of mutagenicity was linked with an absence of carcinogenicity.

MX was reported to induce 2800–13000 revertants/nmol in the *Salmonella typhimurium* TA100 without metabolic activation [Ishiguro et al., 1988; LaLonde et al., 1991], indicating that the compound is one of the most potent mutagens in TA100. The contribution of MX to the total mutagenicity associated with chlorine-treated tap water was estimated to be 15–57% in Finland [Kronberg and Vertiainen, 1988], 15–34% in the United States [Meier et al., 1987a], and 7–21% in Japan [Furihata et al., 1992]. MX is also a mammalian cell clastogen [Meier et al., 1987b] and gives rise to specific DNA adducts [Franzen et al., 1998; Munter et al., 1998]. Despite its strong in vitro mutagenicity, MX was only marginally active at inducing nuclear anomalies in the small intestine of mice when given as a single oral dose of 0.37 mmol/kg [Daniel et al., 1991]. Thus, it has been hypothesized that mammalian cells may effectively detoxify chlorohydroxyfuranones, including MX [Daniel et al., 1991; Meier et al., 1996]. In fact, it has been shown that MX is efficiently inactivated by endogenous defensive systems such as those involving glutathione and cysteine [LaLonde and Xie, 1993; Watanabe et al., 1994]. The results of the present study support the conclusion that such defensive systems could be sufficient to detoxify MX ingested in drinking water at concentrations well above environmental levels [Melnick et al., 1997]. A recent study [Huuskonen et al., 2003] showing no teratogenicity in rats receiving up to 60 ppm MX also supports this hypothesis.

Potentially relevant to our findings is Thilly's [2003] challenge to the hypothesis that environmental chemicals induce a substantial fraction of human point mutations. Thilly's interpretation, based on direct measurements of the kinds and numbers of point mutations in human tissues, rests on the fact that no clear relationship has been established between mutation and exposure to environmental chemical and physical agents, except for sunlight–induced mutations in the skin. He suggested an alternative hypothesis that point mutations arise in tumors of exposed organisms as errors in replication of undamaged DNA during exposure to chemicals that select these initiated cells rather than induce onco-mutations. In other words, these "carcinogens" are actually tumor promoters acting epigenetically, rather than direct mutagens [Trosko, 1997].

In the present study, it was demonstrated that MX inhibited cell–cell communication in WB cells, which is in line with a previous report of weak inhibitory effects on metabolic cooperation in cultured Chinese hamster lung V79 cells [Matsumura et al., 1994]. Our results suggest that MX may inhibit intercellular communication in both liver and bile duct cells of rats, because rat WB cells of oval cell origin, with the potential to differentiate into either cell type, were employed here. Regarding the time course, the peaks at 2 and 10 hr suggest that there is transient inhibition due to post-translational mechanisms, but then a later reduction of expression of connexin genes, such as the gene encoding Cx43, occurs. Most tumor promoters, both complete carcinogens and pure tumor pro-